

Research Papers

Robust bidding strategy of battery energy storage system (BESS) in joint active and reactive power of day-ahead and real-time markets



Mohammad Farahani, Abouzar Samimi*, Hossein Shateri

Department of Electrical Engineering, Arak University of Technology, Arak, Iran

ARTICLE INFO

Keywords:

Joint active/reactive power market
Robust Optimization
Energy storage system
Day ahead market
Real-time market

ABSTRACT

The most important applications of an Energy Storage System (ESS) in power systems are energy arbitrage along with procurement of Ancillary Services (ASs). In addition to economic benefits, ESS also improves network reliability and stability. In this paper, a bidding strategy model of a Battery Energy Storage System (BESS) in a Joint Active and Reactive Power Market (JARPM) in the Day-Ahead-Market (DAM) and the Real-Time-Market (RTM) using a robust framework is presented. In this study, the BESS model is considered a price-taker, with the private owner trying to maximize its profit while facing price uncertainty. In the first stage of the proposed model, JARPM is cleared in a deterministic way without the presence of BESS to determine hourly prices of active and reactive power. In the second stage, by determining the prices uncertainty interval and the robust budget for DAM and RTM, the robust bidding model aims to maximize the BESS owner's profit, using the robust counterpart formation of the objective function and dual theory. The proposed robust formulation based on a Mixed Integer Non-Linear Programming Model (MINLP) is implemented in the GAMS software environment on the IEEE-24-RTS test system. The result shows that by the participation of BEES in the market, the average price of active and reactive power is reduced by 2% & 3% respectively. In addition, the overall cost of DAM execution is reduced markedly. On the other hand, the proposed framework in three case studies also guarantees a suitable profit level for the private owners of BESS (30–35 \$/hour).

1. Introduction

1.1. Literature review

The electricity industry has recently evolved from a centralized framework to a competitive and deregulated structure and aims to promote efficient utilization of power systems and ensure the quality of providing electricity at the lowest possible cost. Ancillary Services (ASs) are services required by the Independent System Operator (ISO) to transmit active power securely and stably. Reactive power is considered one of the most essential ASs in power systems. Traditional producers in power systems, such as Synchronous Generators (SGs), and new market players (including Distributed Generators (DGs), responsive loads, and aggregators on behalf of their clients, i.e., small loads and electric vehicles) can profit from effective participation in reactive power markets. Sufficient provision of reactive power is vital in improving the system's voltage stability and alleviating transmission lines' congestion, reducing power losses and operational costs. Previous researches on reactive power markets have generally proposed two models for reactive market

settlement: the Separate Reactive Power Market (SRPM) framework and Joint Active and Reactive Power Market (JARPM) model. The SRPM will be executed after clearing the active power market. Balancing markets compensate for imbalances caused by the compulsion to reduce/increase active power generation to satisfy the reactive power requirements. Irrespective of the relatively complex implementation of the JARPM, it considers the interactions between active and reactive power, including the AC power flow equations, branch loading limits, and the capability curves for each reactive provider, such as SGs, to achieve a less costly and more efficient solution compared to the SRPM model. Authors in [1] have proposed real-time reactive power pricing based on Lagrange coefficients based on an Optimal Power Flow (OPF) solution. Apart from that, the effect of voltage and congestion constraints on reactive power pricing has been investigated. The SGs, the main producer of reactive power in the power system, develop the basis of a competitive reactive market based on the Expected Payment Function (EPF) concept [2]. In Ref. [3], local reactive power markets in separate voltage control areas have been investigated considering the local nature of reactive power provision. Lost Opportunity Cost (LOC), as one of the most critical components of both JARPM and SRPM, refers to a

* Corresponding author.

E-mail address: abouzarsamimi@alumni.iust.ac.ir (A. Samimi).

Nomenclature	
Acronyms	
ARO	Adaptive Robust Optimization
AS	Ancillary Service
BESS	Battery Energy Storage System
CAES	Compressed Air Energy Storage
DAM	Day Ahead Market
DER	Distributed Energy Resource
DG	Distributed Generation
DR	Demand Response
DRO	Distributionally Robust Optimization
DSO	Distribution System Operator
EPF	Excepted Payment Function
ESS	Energy Storage System
IGDT	Information Gap Decision Theory
ISO	Independent System Operator
JARPM	Joint Active and Reactive Power Market
LAES	Liquid Air Energy Storage
LOC	Lost Opportunity Cost
LP	Linear Programming
MC	Market Cost
MCP	Market-Clearing Price
MINLP	Mix Integer Non-Linear Programming
MIP	Mix Integer Linear Programming
OPF	Optimal Power Flow
PV	PhotoVoltaic
RES	Renewable Energy Source
RO	Robust Optimization
RTM	Real-time market
SG	Synchronous Generator
SOC	State of Charge
SRPM	Separate Reactive Power Market
TPF	Total Payment Function
WT	Wind Turbine
<i>Indices, parameters, and variables</i>	
h	time interval index (1 to 24)
i, j	bus indices
n	trapezoid index (1 to N^{trap})
g	generator index (1 to g_b)
s	BESS index
$S_{i,j}^{max}$	maximum permissible loading of the line between bus i and bus j
V_{max}, V_{min}	maximum and minimum permissible voltage of bus, respectively
P_h, Q_h	total active and reactive power generation in h^{th} time interval, respectively
P_h^i, Q_h^i	active and reactive load of i^{th} bus in h^{th} time interval, respectively
P_h^g, Q_h^g	generated active and reactive power of the generator g connected to bus i in h^{th} time interval, respectively
P_g^{min}, P_g^{max}	minimum and maximum active power generation of the SG g , respectively
δ_i, h	the voltage angle of bus i in h^{th} time interval
θ_{ij}	the angle of admittance between bus i and bus j
$X_s^{i,g}$	synchronous reactance of SG g connected to bus i in h^{th} time interval
$V_t^{i,g}$	terminal voltage of SG g connected to bus i in h^{th} time interval
$E_{af}^{i,g}, h$	Internal voltage of SG g connected to bus i
$I_a^{i,g}$	armature current of SG g connected to bus i in h^{th} time interval
$Q_1^{i,g}, h, Q_2^{i,g}$ and $Q_3^{i,g}, h$	the reactive power of SG g connected to bus i in h^{th} time interval in operating regions of absorption,
$EPF_h^{i,g}$	injection, and lost opportunity, respectively
Q_{Base}	EPF of SG g connected to bus i in h^{th} time interval
TPF_h	reactive power requirement of the internal equipment of SG
$a_0^{i,g}$	total payment function for reactive power in h^{th} time interval
$m_1^{i,g}, m_2^{i,g}$	the offered cost of SG for availability
$m_3^{i,g}, Q_h^{i,g}$	the offered cost of losses of SG g connected to bus i operation in the reactive power absorption and injection region, respectively
$W_0^{i,g}, W_1^{i,g}, W_2^{i,g}$ and $W_3^{i,g}$	binary variables related to EPF of SG g connected to the bus i in h^{th} time interval
$W_{P,s}^{i,g}$	binary variable indicating whether the bid of SG g connected to bus i in h^{th} time interval is accepted or not in the active power market
$\rho_{0,h}$	MCP for the availability component in h^{th} time interval
$\rho_{1,h}, \rho_{2,h}, \rho_{3,h}$	MCP for the losses component in absorption and injection regions as well as the opportunity component in h^{th} time interval
ρ_p, h	MCP for active power in h^{th} time interval
Q_{pr}, h	reactive power price in h^{th} time interval
MC_h	market cost in h^{th} time interval of the market
$E_{s,0,i}, E_{s,24,i}$	initial and final SOC of BESS s connected to bus i , respectively
$E_{s,h,i}$	SOC of BESS s connected to bus i in h^{th} time interval
$SB_{s,i}^{rated}$	rating power of BESS s connected to bus i
$P_{s,h,i}, Q_{s,h,i}$	total active and reactive power of BESS s connected to bus i in h^{th} time interval, respectively
$p_n^{s,h,i}, q_n^{s,h,i}$	active and reactive power of n^{th} trapezoid of BESS s connected to bus i in h^{th} time interval, respectively
$P_{n,r}^{s,i}, P_{n,l}^{s,i}$	active power of the right and left corners of the n^{th} trapezoid of BESS s connected to bus i , respectively
$Q_{n,r}^{s,i}, Q_{n,l}^{s,i}$	reactive power of the right and left corners of the n^{th} trapezoid of BESS s connected to bus i , respectively
$a_n^{s,h,i}$	binary variable related to n^{th} trapezoid of BESS s connected to bus i in the h^{th} time interval (1 for selected and 0 for unselected)
$pch_n^{s,h,i}, pdis_n^{s,h,i}$	active power charge and discharge of n^{th} trapezoid related to BESS s connected to bus i in h^{th} time interval, respectively
$qch_n^{s,h,i}, qdis_n^{s,h,i}$	charge and discharge the reactive power of n^{th} trapezoid related to BESS s connected to bus i in h^{th} time interval, respectively
$IP_{s,h,i}^{ch}, IP_{s,h,i}^{dis}$	binary variables used to prevent simultaneous charge and discharge of active power of BESS s connected to bus i in h^{th} time interval, respectively
$IQ_{s,h,i}^{ch}, IQ_{s,h,i}^{dis}$	binary variables used to prevent simultaneous charge and discharge of reactive power of BESS s connected to bus i in h^{th} time interval, respectively
$\eta_{s,i}^{ch}, \eta_{s,i}^{dis}$	charge and discharge efficiency of the BESS s connected to bus i , respectively
$P_{s,h,i}^{DAM, ch}, P_{s,h,i}^{DAM, dis}$	active power of charge and discharge of BESS s connected to bus i in h^{th} time interval in DAM, respectively
$P_{s,h,i}^{RTM, ch}, P_{s,h,i}^{RTM, dis}$	active power of charge and discharge of BESS s connected to bus i in h^{th} time interval in RTM, respectively
$Q_{s,h,i}^{DAM, ch}, Q_{s,h,i}^{DAM, dis}$	reactive power of charge and discharge of BESS s connected to bus i in h^{th} time interval in DAM, respectively
$Q_{s,h,i}^{RTM, ch}, Q_{s,h,i}^{RTM, dis}$	reactive power of charge and discharge of BESS s connected to bus i in h^{th} time interval in RTM, respectively
$\alpha_{DAM,P}, \alpha_{RTM,P}$	uncertainty intervals of active power price in DAM and RTM, respectively
$\beta_{DAM,Q}, \beta_{RTM,Q}$	uncertainty intervals of reactive power price in DAM

and RTM, respectively

$\Gamma_{DAM}^{s,i}, \Gamma_{RTM}^{s,i}$ robust budgets of BESS s connected to bus i in the DAM and RTM, respectively

$Z_{0,h}^{s,i}, a_{s,h,i}$ dual variables of active power of BESS s connected to bus i in h^{th} time interval in RTM

$Y_{0,h}^{s,i}, b_{s,h,i}$ dual variables of reactive power of BESS s connected to bus i in h^{th} time interval in RTM

$W_{0,h}^{s,i}, c_{s,h,i}$ dual variables of active power of BESS s connected to bus i in h^{th} time interval in DAM

$X_{0,h}^{s,i}, d_{s,h,i}$ dual variables of reactive power of BESS s connected to bus i in h^{th} time interval in DAM

$z_{s,h,i}, y_{s,h,i}$ active and reactive power auxiliary variables of BESS s

connected to bus i in h^{th} time interval in RTM, respectively

$w_{s,h,i}, x_{s,h,i}$ active and reactive power auxiliary variables of BESS s connected to bus i in h^{th} time interval in DAM, respectively

$\pi_{max,h}^{DAM}, \pi_{min,h}^{DAM}$ maximum and minimum forecasted active power price in h^{th} time interval in DAM, respectively

$\pi_{max,h}^{RTM}, \pi_{min,h}^{RTM}$ maximum and minimum forecasted active power price in h^{th} time interval in RTM, respectively

$q_{max,h}^{DAM}, q_{min,h}^{DAM}$ maximum and minimum forecasted reactive price in h^{th} time interval of DAM, respectively

$q_{max,h}^{RTM}, q_{min,h}^{RTM}$ maximum and minimum forecasted reactive price in h^{th} time interval of RTM, respectively

decrease in the sale of electrical energy in the energy market due to the need for providing reactive power or other ASs. In [4], a modified triangular pricing method for reactive power has been compared with LOC. Also, the optimization of JARPM has been addressed using the ant colony algorithm. In [5], Wind Turbines (WTs) as one of the most important Renewable Energy Resources (RESs) can be investigated as a reactive power provider under the EPF concept. In this reference, the authors have proposed a new method to calculate the LOC for WT by considering hourly wind fluctuations. Considering the growth of wind generation in power systems, the necessity of accurate prediction of the available power of these resources is undeniable [6]. This reference presents a new model to predict WT power based on empirical analysis, feature selection, and a combined prediction tool. With regard to ASs, [7] have introduced an appropriate pricing framework for different reserve types (up- down/generation-demand) based on Location Marginal Pricing (LMP) and considering the LOC. Reactive power modeling and pricing Distributed Energy Resources (DERs) have been discussed in [8]. The impact of the probability of various network contingencies on reactive power prices has been analyzed in [9]. MCP or uniform payment, Pay-As-Bid (PAB), and Vickery auction are among the different solutions for market settlement. The authors in [10] have investigated these frameworks in the energy market by introducing a model based on ant colony optimization. The volatility of prices, average settlement price, and allocation efficiency are computed as evaluation criteria. By ranking frameworks based on Principal Component Analysis (PCA), the authors prove that the MCP method with only one bid block has the highest priority. In [11], the optimal scheduling of RESs, tap-changers, and capacitor banks has been formulated based on the JARPM at the distribution level. Moreover, in [12], a simultaneous active and reactive power market has been introduced for smart distribution systems in the presence of dispatchable DGs, Demand Response (DR), and RES. In [13], the JARPM for active distribution systems has been investigated by considering uncertainties of wind generation and system loads using weibull and gaussian distributions in a Stochastic Programming (SP) framework. Roulette wheel mechanism, probability distribution function discretization and lattice monte carlo simulation have been used to model uncertainty of DERs. The main difference between the DAM and RTM pertains to offline scheduling of DAM and online operation of RTM [14]. The price difference in various hours of market leads to need for participation of ESSs and shiftable loads in the network. Authors in ref. [15] have reviewed the challenges of the reactive power market. Ref. [16] has reviewed all aspects of the electricity market, bidding strategy challenges, and recent market optimization techniques. Moreover, the authors have proposed a new optimization model based on harris hawk optimization neural network by guaranteeing convergence with high speed compared to other evolutionary algorithms.

Network contingencies and the presence of intermittent renewable sources have led to uncertainty entering the decision-making and operation of the power system. The probabilistic methods, feasibility process, hybrid methods (probability and feasibility), distance-based analysis, Robust Optimization (RO), and the Information Gap Decision

Theory (IGDT) are some common methods for uncertainty modeling [17]. RO is known as a solution in analyzing optimization problems under the effect of uncertainties and insufficient information about the nature and probability distribution of uncertain parameters [18]. A RO approach finds an optimal decision that optimizes its performance in the worst case of uncertainties, and the obtained solution is feasible for all uncertainty situations. RO has acceptable performance in several areas of the power systems: Energy Hub (EH) management [19], unit commitment for minimizing wind spillage and load shedding [20], optimal adjustment of power system stabilizer [21], management of a joint active and reactive and reserve scheduling of a smart microgrid and robust power system planning considering CO₂ emissions [22]. In RO, two sets of decision variables are defined [23]: design variables (here and now) - control variables (wait and see). The growth rate of power system demand, fuel cost, and the amount of energy available from RESs are among the uncertainties that authors of [23] have modeled using RO. The ultimate goal is to find robust long-term expansion planning with the lowest possible cost for the generation/transmission network. The proposed model is two-stage and non-recursive, and the simulation results on large and small networks show the satisfactory performance of the model in the face of network uncertainties and contingency. Ref. [24] has used IGDT to plan EH with uncertainty caused by the behavior of loads. In [25], unit commitment problem with uncertainties of market prices and RES units, electrical and thermal loads and the energy of ESS in charging stations has been formulated. Ref. [26] introduces a two-stage planning framework for optimal use of EH in the worst scenarios and compares it with SP model. In [27], auto regressive integrated moving average model is used to generate valid scenarios for RTM prices and WT generation, while normal PDF is implemented to model the load uncertainty. In [28], the participation of plug-in hybrid electric vehicles in the market has been analyzed based on the RO technique considering price uncertainty, and it has been confirmed that centralized management of plug-in hybrid electric vehicle charging can lead to lowering costs. In the literature, two types of RO have been used in power system studies: recursive RO (three-stage) and non-recursive RO (two-stage). In [29], based on ESSs at the microgrid level, the uncertainties of load and DGs have been handled using decision theory. Authors in [30] have proposed a model that use the IGDT approach to optimize the bidding curve of intelligent parking lots. Aggregation of consumer responses and exchange with the upstream network (wholesale market) through DR programs are the main tasks of the DR aggregator. In [31], the participation rate of consumers is modeled using SP and the uncertainty of market prices with RO. This reference has also considered an ESS under the ownership of the aggregator in different budgets and robust uncertainty intervals. In [32], a two-stage optimization model has been proposed to scheduling ESSs by considering the uncertainties of loads, price and generation of solar systems as a main renewable resource of energy. Both Benders decomposition method and the Cutting-Plane-Algorithm (CPA) have been used in [33] to achieve a robust settlement of a simultaneous energy and reserve market. In [34], the energy market has been settled through combined modeling the

Table 1
Taxonomy of recent works in the area.

Ref.	RTM uncertainty	DAM uncertainty	RTM	DAM	ESS
[43]	x	SP	x	✓	CAES
[48]	x	x	✓	✓	CAES
[49]	x	SP	x	✓	BESS
[50]	x	SP	x	✓	BESS
[51]	x	RO	x	✓	CAES
[52]	SP	SP	✓	✓	BESS
[41]	SP	SP	✓	✓	BESS
[40]	SP	SP	✓	✓	BESS
[53]	x	SP	x	✓	BESS
[39]	x	RO	x	✓	BESS
[54]	x	RO	x	✓	CAES
[38]	x	RO	x	✓	BESS
[55]	x	x	✓	✗	LAES
[56]	RO	SP	✓	✓	BESS
This paper	RO	RO	✓	✓	BESS

uncertainty of the RTM prices based on the RO method and the uncertainty of DAM prices using SP. In [14], a day-ahead energy market model with spatial-temporal pricing of players, including DERs, BESSs, and RESs, has been presented using recursive three-stage Adaptive RO (ARO). In [35], a self-scheduling of hydro-thermal units in a smart grid has been studied using the robust counterpart formulation and a duality concept. In [36], various RO models have been explored and compared, including ordinary RO, ARO, Distributionally RO (DRO), and their solution methods.

ESSs are well known as one of the most effective ways to reduce the imbalance between generation and consumption. The development of ESSs was related to deploying the Pumped-Storage Hydropower (PSH) systems in Europe for load leveling [37]. With the ever-increasing penetration of RESs, the need to integrate ESSs into electric systems to tackle the existing uncertainties has received significant attention. With the advancement of energy storage technologies in the last decade, it has been possible to increase their capacity and reduce relevant costs. An energy market based on a robust framework presented in [38] not only ensures ESS profit but also reduces network losses. Battery energy storage systems (BESSs) are expected to grow by 12 GW by 2024 [39]. In [40], a model has been proposed in DAM and RTM based on SP that helps to raise ESS profit using LP and Mixed-Integer Linear

Programming (MIP) models. In [41], an optimal bidding strategy for participation of price-taker ESS in the DAM is modeled. Authors in [42] examine the impact of ESS and DR in the long-term planning of power systems based on a two-level problem. The optimal location and sizing of ESSs at the upper level and the optimal planning of the power network are determined at the lower level. Ref. [43] has modeled the maximization of the expected profit of CAES with a combination of SP and RO. In [45], an optimal power allocation approach is introduced for power systems equipped with PV, WT, and lead-acid battery based on an intelligent evolutionary algorithm (modified shark-smelling optimization). Ref. [46] has proposed a dynamic model to achieve a reliable operation in distribution systems by considering different types of commercial, residential, and industrial loads and their prioritization in different climatic scenarios. Two primary goals of optimization problem presented in [47] are minimization of installation, operation, and maintenance costs of ESSs as well as reducing pollution caused by traditional energy sources in an islanded hybrid system. Table 1 lists some important relevant references in which ESS bidding models are studied.

1.2. Motivation

Despite extensive research on ESS, its role in the markets as an independent actor has never been studied. In other words, none of the previous references address the potential of participation of ESSs with private sector owners in the DAM and RTM of active and reactive power considering price uncertainty. Therefore, this paper presents a bidding strategy model of a BESS in a JARPM in the DAM and the RTM using a robust framework for the first time. In this study, the BESS model is considered a price-taker, with the private sector's owner trying to maximize its profits in the face of price uncertainty. To this end, the initial hourly prices for active and reactive power are given by clearing DAM without BESS and uncertainty. By defining some specified scenarios on the SGs' generation limits, loads, and constraints of lines, the RTM model is executed to achieve real-time active and reactive power prices for each period. The reactive power capability of a BESS is modeled by the trapezoidal method. The proposed model assumes that battery converter constraints are satisfied. Furthermore, this paper considers that the BESSs have various charging/discharging efficiencies

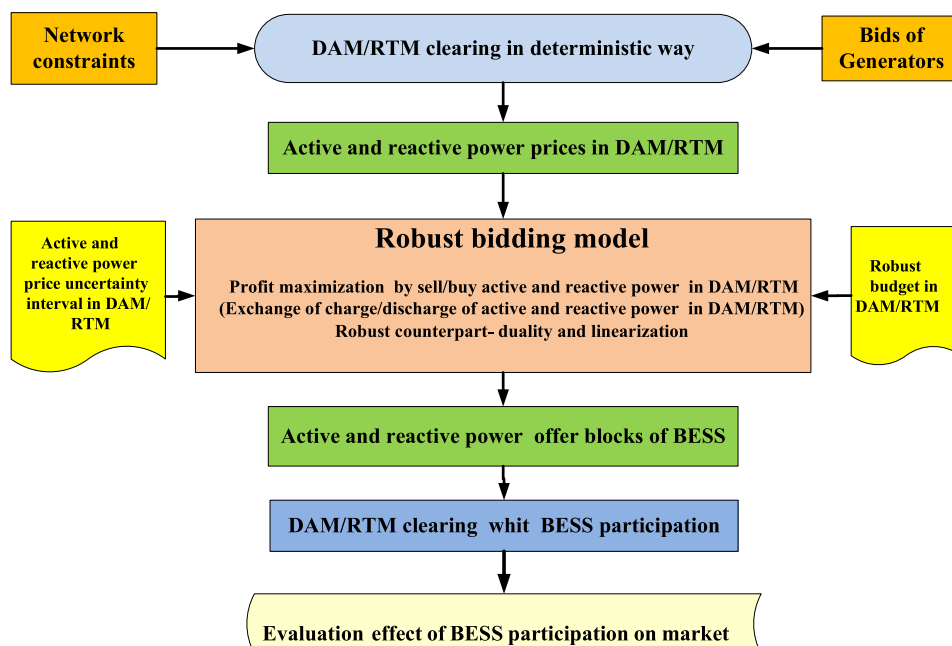


Fig. 1. The overall flowchart for the proposed model.

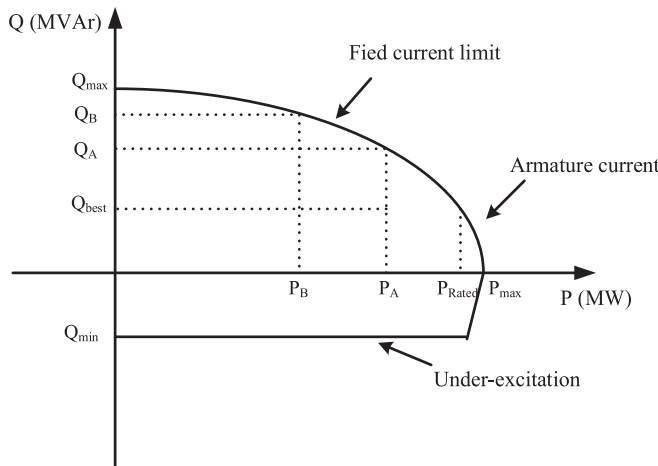


Fig. 2. Capability curve of an SG [42].

along with different robust policies. The proposed robust model is based on a min-max bi-level optimization problem formulated using a robust counterpart and the duality concept to determine the bids of BESS aiming at maximizing its profit. Eventually, the DAM model will be rerun in the presence of BESSs, and accordingly, the effects of the participation of the BESS can be evaluated and analyzed on the market. Fig. 1 illustrates the overall proposed flowchart.

1.3. Contribution

The main innovations of this paper can be summarized as follows:

- To introduce a robust bidding structure in both DAM and RTM for a BESS to maximize its profit considering market price uncertainty.
- To consider BESS's ability to support reactive power using the trapezoidal model.
- To present and analyze a model for a JARPM in the presence of BESS with a private sector owner.

1.4. Paper organization

The paper is structured as follows: Section 2 formulates the JARPM model and its constraints.

Section 3 presents BESS modeling and examines the active and reactive power bid/offer mechanism. Section 4 presents the simulation results of the proposed model. Finally, section 5 summarizes the conclusion and future works.

2. Problem formulation

In this section, separate active and reactive power markets have been introduced. Then, the proposed robust market framework is formulated based on the objective function and constraints related to the JARPM structure.

2.1. Objective function of the active power market

In the separate active power market or energy market, all SGs offer their generation bids in any period to the market as specific blocks (active power - price). ISO settles the market based on an optimization problem to minimize operation costs with regard to the constraints of the system and generators. This paper uses the uniform settlement price auction method based on the MCP concept. The objective function used to settle the active power market is stated in Eq. (1):

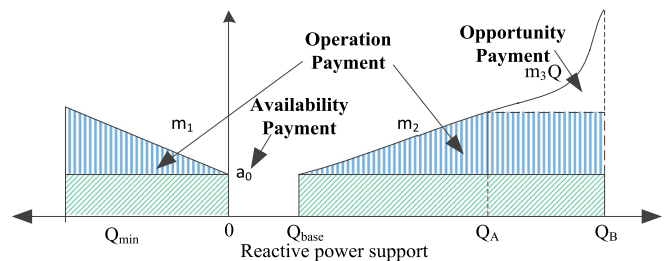


Fig. 3. EPF structure of an SG [9].

$$\min \sum_{h=1}^{24} \sum_{i=1}^{\text{Bus}} \sum_{g=1}^{gb} W_{P,h}^{i,g} \rho_{P,h} P_h^{i,g} \quad (1)$$

The binary variable \$W_{P,h}^{i,g}\$ indicates whether the bid of generator \$g\$ connected to bus \$i\$ in \$h^{th}\$ time interval is accepted or not in the active power market. \$\rho_{P,h}\$ is the active power MCP in \$h^{th}\$ time interval and \$P_h^{i,g}\$ is the active power the generator is committed to supplying in \$h^{th}\$ time interval.

2.2. Objective function of SRPM

The reactive power demand of the network should be provided appropriately so that the generator can meet its active power contract obligations. The output of a separate active power market is made available as the input information of the reactive power market. The EPF of each SG is determined based on the reactive power capability curve, as shown in Fig. 2.

The main constraints of the capability curve of an SG include the limitation of the armature current in Eq. (2), the field current in Eq. (3), and the under-excitation limit of the SG.

$$Q_h^{i,g} \leq \sqrt{\left(V_{\text{terminal},h}^{i,g} I_{a,h}^{i,g}\right)^2 - \left(P_h^{i,g}\right)^2} \quad (2)$$

$$Q_h^{i,g} \leq \sqrt{\left(V_{t,h}^{i,g} \frac{E_{af,h}^{i,g}}{X_{s,h}^{i,g}}\right)^2 - \left(P_h^{i,g}\right)^2 - \left(\frac{V_{t,h}^{i,g}}{X_s^{i,g}}\right)^2} \quad (3)$$

where, \$X_s^{i,g}\$, \$V_{t,h}^{i,g}\$, and \$I_{a,h}^{i,g}\$ show synchronous reactance, generator terminal voltage, and armature current of the SG, respectively. The EPF can be formulated based on the operating point [2]:

According to Eq. (4), the EPF of each SG can be considered as Fig. 3. The EPF is divided into three main components: the cost of losses in the injection region, the cost of losses in the absorption region, and LOC. The coefficients in Eq. (4) constitute different parts of reactive power support costs [2]:

$$EPF_h^{i,g} = a_0^{i,g} + \int_{Q_{\min}}^0 m_1^{i,g} dQ_h^{i,g} + \int_{Q_{\text{Base}}}^{Q_A} m_2^{i,g} dQ_h^{i,g} + \int_{Q_A}^{Q_B} (m_3^{i,g} Q_h^{i,g}) dQ_h^{i,g} \quad (4)$$

In Eq. (4), the coefficients are as follows:

\$a_0^{i,g}\$ is the offered cost of SG for availability (in \\$).

\$m_1^{i,g}\$ is the offered cost of losses resulting from the generator operation in the reactive power absorption region (under excitation mode) \$Q_{\min} \leq Q_1 \leq 0\$ (in \\$/MVAr-h).

\$m_2^{i,g}\$ is the offered cost of losses due to operating in the reactive power injection region \$Q_{\text{Base}} \leq Q_2 \leq Q_A\$ in \\$/MVAr-h).

\$m_3^{i,g} Q_h^{i,g}\$ is the offered opportunity cost for operation in the region \$Q_A \leq Q_3 \leq Q_B\$ (in \\$/MVAr-h)².

The goal of executing a Separate Reactive Power Market is to provide reactive power required by the system to satisfy voltage and security constraints at the lowest possible cost. The total amount of ISO payments to generators, also known as the total payment function (TPF), is expressed in Eq. (5).

$$TPF = \min \sum_{h=1}^{24} \sum_{i=1}^{\text{Bus}} \sum_{g=1}^{gb} \left(\begin{array}{l} W_{0,h}^{i,g} \rho_{0,h} (Q_{\max}^{i,g} - Q_{\min}^{i,g}) \\ -W_{1,h}^{i,g} \rho_{1,h} Q_{1,h}^{i,g} \\ +W_{2,h}^{i,g} \rho_{2,h} (Q_{2,h}^{i,g} - Q_{\text{Base}}^{i,g}) \\ +W_{3,h}^{i,g} \rho_{2,h} (Q_{3,h}^{i,g} - Q_{\text{Base}}^{i,g}) \\ +0.5 W_{3,h}^{i,g} \rho_{3,h} \left((Q_{3,h}^{i,g})^2 - (Q_{\text{Base}}^{i,g})^2 \right) \end{array} \right) \quad (5)$$

Eq. (5) divides the amount of reactive power support into $Q_{1,h}^{i,g}$, $Q_{2,h}^{i,g}$ and $Q_{3,h}^{i,g}$ which respectively indicate the operating point in ($Q_{\min} - 0$), (Q_{Base} to Q_A) and (Q_A to Q_B). The binary variable $W_{0,h}^{i,g}$ only carries a value of 1 if the generator g that is connected to the bus i is accepted in the h^{th} time interval of the market. Each of the binary variables $W_{1,h}^{i,g}$, $W_{2,h}^{i,g}$ and $W_{3,h}^{i,g}$ indicate whether or not the generator's bid is accepted in the relevant area ($Q_{1,h}^{i,g}$, $Q_{2,h}^{i,g}$ and $Q_{3,h}^{i,g}$).

2.3. JARPM objective function

The objective function of JARPM is expressed as Eq. (6). This market ultimately aims to simultaneously minimize the total costs of active power and reactive power at all hours.

$$\min \sum_{h=1}^{24} \left[\sum_{i=1}^{\text{Bus}} \sum_{g=1}^{gb} W_{P,h}^{i,g} \rho_{P,h} P_h^{i,g} + \sum_{i=1}^{\text{Bus}} \sum_{g=1}^{gb} \left(\begin{array}{l} W_{0,h}^{i,g} \rho_{0,h} (Q_{\max}^{i,g} - Q_{\min}^{i,g}) \\ -W_{1,h}^{i,g} \rho_{1,h} Q_{1,h}^{i,g} \\ +W_{2,h}^{i,g} \rho_{2,h} (Q_{2,h}^{i,g} - Q_{\text{Base}}^{i,g}) \\ +W_{3,h}^{i,g} \rho_{2,h} (Q_{3,h}^{i,g} - Q_{\text{Base}}^{i,g}) \\ +0.5 W_{3,h}^{i,g} \rho_{3,h} \left((Q_{3,h}^{i,g})^2 - (Q_{\text{Base}}^{i,g})^2 \right) \end{array} \right) \right] \quad (6)$$

2.4. Constraints of the JARPM

The optimization of the objective function of Eq. (6) should be minimized under constraints (7) to (24).

$$\sum_{g=1}^{gb} P_h^{i,g} - P_h^{i,d} = \sum_{j=1}^{\text{Bus}} |V_{i,h}| |V_{j,h}| |Y_{ij}| \cos(\delta_{i,h} - \delta_{j,h} - \theta_{ij}) \quad (7)$$

$$\sum_{g=1}^{gb} Q_h^{i,g} - Q_h^{i,d} = \sum_{j=1}^{\text{Bus}} |V_{i,h}| |V_{j,h}| |Y_{ij}| \sin(\delta_{i,h} - \delta_{j,h} - \theta_{ij}) \quad (8)$$

$$S_{i,j} < S_{i,j}^{\max} \quad (9)$$

$$V_i^{\min} \leq V_{i,h} \leq V_i^{\max} \quad (10)$$

where, $P_h^{i,d}$ and $Q_h^{i,d}$ respectively represent the hourly active and reactive load of i^{th} bus, $\delta_{i,h}$ and $\delta_{j,h}$ show the voltage angle of bus i and bus j in h^{th} time interval of the market, and θ_{ij} is the angle of admittance between bus i and bus j . Maximum permissible line loading between bus i and bus j is indicated with $S_{i,j}^{\max}$, and the maximum and minimum permissible voltage of buses are respectively determined by V_i^{\max} and V_i^{\min} . Constraints (7) and (8) indicate each bus's load flow and power balance limitation. Constraints (9) and (10) determine the power flow limitation

of transmission lines and the permissible voltage range of buses. Eqs. (11) to (19) indicate the active and reactive power provision constraints of SGs [57]:

$$P_g^{\min} \leq P_h^{i,g} \leq P_g^{\max} \quad (11)$$

$$W_{0,h}^{i,g}, W_{1,h}^{i,g}, W_{2,h}^{i,g}, W_{3,h}^{i,g} \in \{0, 1\} \quad (12)$$

$$Q_h^{i,g} = Q_{1,h}^{i,g} + Q_{2,h}^{i,g} + Q_{3,h}^{i,g} \quad (13)$$

$$W_{2,h}^{i,g} Q_{\text{Base},G}^{i,g} \leq Q_{2,h}^{i,g} \leq W_{2,h}^{i,g} Q_{A,h}^{i,g} \quad (14)$$

$$W_{1,h}^{i,g} Q_{\min}^{i,g} \leq Q_{1,h}^{i,g} \leq 0 \quad (15)$$

$$W_{2,h}^{i,g} Q_{\text{Base}}^{i,g} \leq Q_{2,h}^{i,g} \leq W_{2,h}^{i,g} Q_{A,h}^{i,g} \quad (16)$$

$$W_{3,h}^{i,g} Q_{A,h}^{i,g} \leq Q_{3,h}^{i,g} \leq W_{3,h}^{i,g} Q_{\max}^{i,g} \quad (17)$$

$$W_{1,h}^{i,g} + W_{2,h}^{i,g} + W_{3,h}^{i,g} \leq 1 \quad (18)$$

$$W_{0,h}^{i,g} = W_{1,h}^{i,g} + W_{2,h}^{i,g} + W_{3,h}^{i,g} \quad (19)$$

$$W_{P,h}^{i,g} P_h^{i,g} \leq \rho_{P,h} \quad (20)$$

$$W_{0,h}^{i,g} a_0^{i,g} \leq \rho_{0,h} \quad (21)$$

$$W_{1,h}^{i,g} m_1^{i,g} \leq \rho_{1,h} \quad (22)$$

$$(W_{2,h}^{i,g} + W_{3,h}^{i,g}) m_2^{i,g} \leq \rho_{2,h} \quad (23)$$

$$W_{3,h}^{i,g} m_3^{i,g} \leq \rho_{3,h} \quad (24)$$

Eq. (11) indicates the SG's maximum and minimum active power generation. Binary variables in Eq. (12) define accepted generators in each region of absorption, injection, and lost opportunity. Eq. (13) associated the total reactive power produced by each generator with its operating point in any of the three determined regions. Eqs. (14) to (17) define the operating limits of each region. Eq. (18) prevents operating in more than one region. Eq. (19) indicates that if the generator's bid to provide reactive power in each region is accepted, the availability cost is also paid. Constraint (20) expresses the MCP market settlement method. It sets the highest accepted bid as the criterion for ISO payments to all generators accepted in the market. Constraint (21) determines the highest price for the cost of generator availability in the reactive market. Constraints (22) to (24) implement the MCP settlement method for reactive power for each of the three regions, including absorption, injection, and lost opportunity. The prices obtained at this stage are input parameters for the robust bidding model.

3. Robust active and reactive power bidding/offering of BESS modeling

This section first discusses the conventional BESS modeling and its integration with the trapezoidal method to address the reactive power support capability. In the bidding stage, the owner from the private sector needs to collect information about active and reactive power prices in any DAM and RTM period by adopting a risk-aversive and profit-based approach. Then, through introducing RO and applying it to the BESS bid/offer mechanism, the robust BESS bidding/offering model (a charging-discharging mechanism) in DAM and RTM is formulated. The equations of a BESS model are as follows [58] [59]:

$$E_{s,24,i} = E_{s,0,i} \quad (25)$$

$$E_{s,h,i} = E_{s,(h-1),i} + P_{s,h,i}^{ch} * \eta_{s,i}^{ch} - P_{s,h,i}^{dis} / \eta_{s,i}^{dis} \quad (26)$$

$$0 \leq E_{s,h} \leq EB_s^{\text{rated}} \quad (27)$$

$$IP_{s,h,i}^{ch} + IP_{s,h,i}^{dis} \leq 1 \quad (28)$$

$$IQ_{s,h,i}^{ch} + IQ_{s,h,i}^{dis} \leq 1 \quad (29)$$

$$P_{s,h,i}^{dis} \leq IP_{s,h,i}^{dis} * SB_{s,i}^{\text{rated}} \quad (30)$$

$$P_{s,h,i}^{ch} \leq IP_{s,h,i}^{ch} * SB_{s,i}^{\text{rated}} \quad (31)$$

$$Q_{s,h,i}^{dis} \leq IQ_{s,h,i}^{dis} * SB_{s,i}^{\text{rated}} \quad (32)$$

$$Q_{s,h,i}^{ch} \leq IQ_{s,h,i}^{ch} * SB_{s,i}^{\text{rated}} \quad (33)$$

$E_{s,0,1}$ is the primary SOC of BESS at the beginning of the scheduling period. According to Eq. (25), the same SOC must be reached at the end of the period. $E_{s,h,i}$ represents BESS's remaining capacity at h^{th} . According to Eq. (26), the capacity depends on the BESS capacity in the previous period and charging-discharging powers in the current period. Eq. (27) stands for maximum power rating during an hour. Eq. (28) holds that binary variable $IP_{s,h,i}^{ch}$ and $IP_{s,h,i}^{dis}$ are interdependent to prevent simultaneous charge and discharge of active power in a period. $IQ_{s,h,i}^{ch}$ and $IQ_{s,h,i}^{dis}$ function similarly for reactive power in Eq. (29). $\eta_{s,i}^{ch}$ and $\eta_{s,i}^{dis}$ determine the charging/discharging efficiency of the BESS ($\eta_{s,i}^{ch} > \eta_{s,i}^{dis}$). The maximum permissible charge/discharge capacity for active and reactive power at each period is considered equal to the capacity of BESS according to Eqs. (30) to (33). BESS's operating point is selected in one of the four quadrants of the performance curve to maximize the owner's profit based on the binary variables in Eqs. (28)–(29). These regions can be selected as follows:

Region 1: In this mode, the BESS charges or buys active/reactive power. In this zone, the binary variables of the decision-making in Eqs. (28)–(29) are $IP_{s,h,i}^{ch} = 1$, $IP_{s,h,i}^{dis} = 0$, $IQ_{s,h,i}^{ch} = 1$, and $IQ_{s,h,i}^{dis} = 0$.

Region 2: In this situation, the BESS discharges or sells active power and charges reactive power. In this area, the corresponding binary variables are $IP_{s,h,i}^{ch} = 0$, $IP_{s,h,i}^{dis} = 1$, $IQ_{s,h,i}^{ch} = 1$, and $IQ_{s,h,i}^{dis} = 0$.

Region 3: In this region, the BESS discharges active and reactive power. Here, the binary variables are $IP_{s,h,i}^{ch} = 0$, $IP_{s,h,i}^{dis} = 1$, $IQ_{s,h,i}^{ch} = 0$, and $IQ_{s,h,i}^{dis} = 1$.

Region 4: In this mode, The BESS charges active power and discharges reactive power. The binary variables in accordance with this area are $IP_{s,h,i}^{ch} = 1$, $IP_{s,h,i}^{dis} = 0$, $IQ_{s,h,i}^{ch} = 0$, and $IQ_{s,h,i}^{dis} = 1$.

3.1. Linearization of the capability curve of BESS

In this paper, the capability curve of BESS has been linearized to reduce the computational burden of the problem and address the ability to support the reactive power of a BESS. There are three methods to linearize the active and reactive power performance of the BESS:

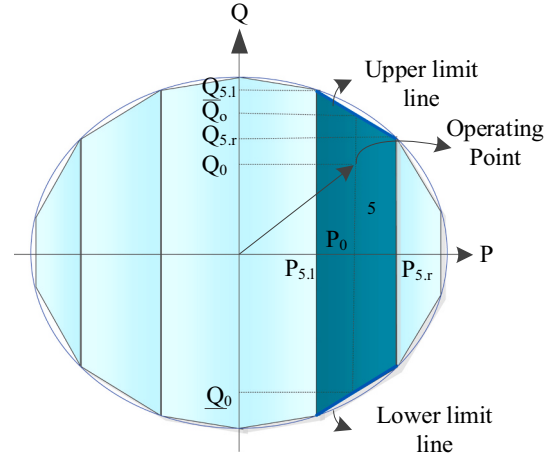


Fig. 4. Approximation of BESS PQ-circle based on trapezoidal-based technique [62].

$$P_{s,h,i} = \sum_{n \in N^{\text{trap}}} p_n^{s,h,i} \quad (34)$$

$$Q_{s,h,i} = \sum_{n \in N^{\text{trap}}} q_n^{s,h,i} \quad (35)$$

$$\alpha_n^{s,h,i} P_{n,l}^{s,i} \leq p_n^{s,h,i} \leq \alpha_n^{s,h,i} P_{n,r}^{s,i} \quad (36)$$

$$-\bar{Q}_{n,r}^{s,i} - \frac{Q_{n,r}^{s,i} - Q_{n,l}^{s,i}}{P_{n,r}^{s,i} - P_{n,l}^{s,i}} (P_{s,h,i} - P_{n,l}^{s,i}) \leq q_n^{s,h,i} \leq \bar{Q}_{n,l}^{s,i} + \frac{Q_{n,r}^{s,i} - Q_{n,l}^{s,i}}{P_{n,r}^{s,i} - P_{n,l}^{s,i}} (P_{s,h,i} - P_{n,l}^{s,i}) \quad (37)$$

$$\sum_{n \in N^{\text{trap}}} \alpha_n^{s,h,i} = 1 \quad (38)$$

$$p_n^{s,h,i} = p_{ch,n}^{s,h,i} + p_{dis,n}^{s,h,i} \quad (39)$$

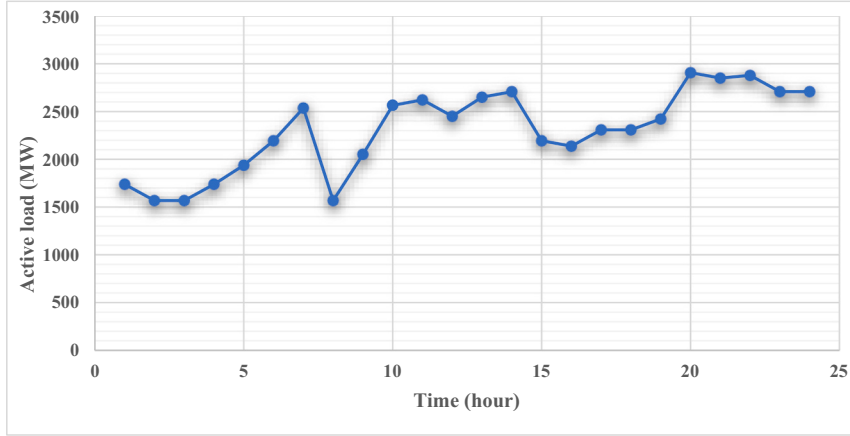
$$q_n^{s,h,i} = q_{ch,n}^{s,h,i} + q_{dis,n}^{s,h,i} \quad (40)$$

1. linearization based on polygonal approximation of PQ-circle [60].
2. linearization based on approximating second-order terms with piecewise linear terms [37] and [61].
3. linearization of PQ-circle based on trapezoidal-based technique [62].

Here, using the method stated in [62], the capability curve of the BESS is linearized based on the trapezoidal method, as shown in Fig. 4. The values of active and reactive power are specified as the right and left corners of the n^{th} trapezoid with l and r subscripts ($P_{n,l}^{s,i}, P_{n,r}^{s,i}, Q_{n,l}^{s,i}$ and $Q_{n,r}^{s,i}$). Eqs. (34) and (35) calculate the total active and reactive power of BESS based on the power of each trapezoid ($p_n^{s,h,i}, q_n^{s,h,i}$). The permissible and satisfactory level of the capability curve of each BESS is covered by six trapezoids. The number of trapezoids is directly associated with the accuracy of the calculation. The binary variable $\alpha_n^{s,h,i}$ represents trapezoid selected in the h^{th} time interval of market according to Eq. (36). Using Eq. (37), the variation of reactive power in each trapezoid is linearly related to the active power. In each period, only one trapezoid can be selected. This requirement is expressed by Eq. (38). According to Eqs. (39) and (40), the power of each trapezoid consists of charge and discharge modes.

3.2. Modeling robust bidding/offering optimization of BESS

Here, the problem of BESS profit maximization is solved using RO method [22] [27] as explained in the following. A function like $z = f(x, y)$ which is linear with respect to x (as uncertain variables) and nonlinear with respect to y (as known values) is considered as the objective function. Here, market prices are uncertain parameters and

**Fig. 5.** Planned Load profile in 24 h.

corresponding required data is not available to determine their Probability Distribution Function. The uncertainty of x is modeled using the concept of uncertainty set $U(x)$ as follows:

$$x \in U(x) = \{x \mid |\bar{x} - \tilde{x}| \leq \hat{x}\} \quad (41)$$

\bar{x} : predicted value \tilde{x} : uncertain value \hat{x} : maximum deviation (uncertainty) from \bar{x} .

The problem therefore can be formulated as follows:

$$\max_y z$$

$$z \leq f(x, y) \quad (43)$$

$$f(x, y) = A(y)^*x + g(y) \quad (44)$$

$$\text{subject to : } x \in U(x) = \{x \mid |\bar{x} - \tilde{x}| \leq \hat{x}\} \quad (45)$$

$A(y)$ is the coefficients matrix of the parameter x (here, active and reactive powers) which is defined as follows:

$$A(y) = \begin{bmatrix} a_1(y) \\ a_2(y) \\ a_3(y) \\ \vdots \\ a_n(y) \end{bmatrix} \quad (46)$$

To solve the problem, the robust counterpart of the problem is formed and analyzed:

$$\max_y z \quad (47)$$

$$z \leq f(x, y) \quad (48)$$

$$f(x, y) = A(y)^*\bar{x} + g(y) - \max_{w_i} \sum_i a_i(y)^*\hat{x}^* w_i \quad (49)$$

$$\sum_i w_i \leq \Gamma \quad (50)$$

$$0 \leq w_i \leq 1 \quad (51)$$

w_i is the coefficients used to model the robust counterpart of the objective function. The main optimization problem can turn into two nested problems as follows:

$$\max_{w_i} (a_1(y)^*\hat{x}_1 \ a_2(y)^*\hat{x}_2, \dots, a_n(y)^*\hat{x}_n) \begin{pmatrix} w_1 \\ w_2 \\ \vdots \\ \vdots \\ w_n \end{pmatrix} \quad (52)$$

$$\begin{pmatrix} 1 & 1 & \dots & 1 \\ 1 & 0 & \dots & 0 \\ 0 & 1 & \dots & 0 \\ \vdots & \vdots & \ddots & \vdots \\ 0 & 0 & \dots & 1 \end{pmatrix} \begin{pmatrix} w_1 \\ w_2 \\ \vdots \\ \vdots \\ w_n \end{pmatrix} \leq \begin{pmatrix} \Gamma \\ 1 \\ 1 \\ \vdots \\ 1 \end{pmatrix} \quad (53)$$

The above problem is linear with respect to w_i and its dual form is as follows:

$$\min_{\alpha_i, Z_0} \sum_i \alpha_i \quad (54)$$

$$Z_0 + \alpha_i \geq a_i(y)^*\hat{x}_i \quad (55)$$

By replacing Eq. (54) in Eq. (47), we have:

$$\max_{y, \alpha_i, Z_0} z \quad (56)$$

$$z \leq f(x, y) \quad (57)$$

$$f(x, y) = A(y)^*\bar{x} + g(y) - \Gamma Z_0 - \sum_i \alpha_i \quad (58)$$

Eqs. (56)–(58) indicate the final model used for the proposed RO problem.

The BESS bidding/offering method can be described as follows: The profit of BESS s connected to bus i for active and reactive power exchange is indicated by the objective function of $profits_s$, as given in Eq. (59). It consists of four chunks: the total costs of exchange active power in DAM and RTM as well as exchange reactive power in DAM and RTM. Furthermore, $\Gamma_{DAM}^{s,i}$ and $\Gamma_{RTM}^{s,i}$ are robust budgets of BESS s connected to bus i in DAM and RTM. Eq. (59) expresses the optimization form of JARPM to operate the robust counterpart. Eqs. (60) to (71) express the duality theory and linearization to solve the problem. $z_{s,h,i}$, $y_{s,h,i}$, $W_{s,h,i}$, $X_{s,h,i}$, $a_{s,h,i}$, $b_{s,h,i}$, $c_{s,h,i}$ and $d_{s,h,i}$ are dual variables of active and reactive power of BESS s connected to bus i in h^{th} time interval of RTM and DAM, respectively.

Table 2

Active and reactive power limits and offers for SGs.

Bus	Generator	Pmax (MW)	Pmin (MW)	bid#1 (\$/MW)	bid#2 (\$/MW)	bid#3 (\$/MW)	bid#4 (\$/MW)	Qmax (MVAr)	Qmin (MVAr)	a0 (\$)	m1 (\$/MVAr-h)	m2 (\$/MVAr-h)	m3 (\$/(MVAr-h) ²)
1	G1	20	16	40	45	50	55	10	0	0.096	0.86	0.86	0.56
	G2	20	16	40	45	50	55	10	0	0.094	0.82	0.82	0.45
	G3	76	15	10	11	12	13	30	-25	0.085	0.79	0.79	0.49
2	G4	76	15	10	11	12	13	30	-25	0.083	0.82	0.82	0.30
	G5	20	16	40	45	50	55	10	0	0.050	0.54	0.54	0.38
	G6	20	16	40	45	50	55	10	0	0.042	0.42	0.42	0.45
7	G7	76	15	10	11	12	13	30	-25	0.069	0.68	0.68	0.39
	G8	76	15	10	11	12	13	30	-25	0.065	0.62	0.62	0.47
	G9	100	25	15	16	17	18.7	60	0	0.075	0.61	0.61	0.53
13	G10	100	25	15	16	17	18.7	60	0	0.080	0.75	0.75	0.36
	G11	100	25	15	16	17	18.7	60	0	0.070	0.65	0.65	0.42
	G12	197	69	18	19	19.5	20.7	230	0	0.068	0.50	0.50	0.41
14	G13	197	69	18	19	19.5	20.7	230	0	0.070	0.54	0.54	0.49
	G14	197	69	18	19	19.5	20.7	230	0	0.075	0.60	0.60	0.50
	SC	-	-	-	-	-	200	-50	0.094	0.81	0.81	-	-
15	G15	12	2	20	21	23	24.1	6	0	0.065	0.60	0.60	0.40
	G16	12	2	20	21	23	24.1	6	0	0.050	0.58	0.58	0.35
	G17	12	2	20	21	23	24.1	6	0	0.060	0.73	0.73	0.38
16	G18	12	2	20	21	23	24.1	6	0	0.055	0.61	0.61	0.37
	G19	12	2	20	21	23	24.1	6	0	0.052	0.50	0.50	0.36
	G20	155	54	8	8.5	9	10	80	-50	0.051	0.51	0.51	0.57
18	G21	155	54	8	8.5	9	10	80	-50	0.050	0.50	0.50	0.50
	G22	400	100	4	4.5	5	5.65	200	-50	0.090	0.85	0.85	0.85
	G23	400	100	4	4.5	5	5.65	200	-50	0.080	0.75	0.75	0.75
22	G24	50	0	0	0	0	0	16	-10	0.042	0.42	0.42	0.27
	G25	50	0	0	0	0	0	16	-10	0.050	0.48	0.48	0.35
	G26	50	0	0	0	0	0	16	-10	0.045	0.42	0.42	0.38
Hydro units	G27	50	0	0	0	0	0	16	-10	0.048	0.44	0.44	0.35
	G28	50	0	0	0	0	0	16	-10	0.049	0.45	0.45	0.43
	G29	50	0	0	0	0	0	16	-10	0.055	0.46	0.46	0.32
23	G30	155	54	8	8.7	9	10	80	-50	0.090	0.85	0.85	0.85
	G31	155	54	8	8.7	9	10	80	-50	0.095	0.89	0.89	0.50

$$\text{Profit}_{s,i} = \min \left[\sum_h Z_{0,h}^{s,i} * \Gamma_{RTM}^{s,i} + \sum_h a_{s,h,i} - \sum_h \pi_h^{RTM} * (P_{s,h,i}^{RTM,dis} - P_{s,h,i}^{RTM,ch}) + \right. \\ \left. \sum_h Y_{0,h}^{s,i} * \Gamma_{RTM}^{s,i} + \sum_h b_{s,h,i} - \sum_h q_h^{RTM} * (Q_{s,h,i}^{RTM,dis} - Q_{s,h,i}^{RTM,ch}) + \right. \\ \left. \sum_h W_{0,h}^{s,i} * \Gamma_{DAM}^{s,i} + \sum_h c_{s,h,i} - \sum_h \pi_h^{DAM} * (P_{s,h,i}^{DAM,dis} - P_{s,h,i}^{DAM,ch}) + \right. \\ \left. \sum_h X_{0,h}^{s,i} * \Gamma_{DAM}^{s,i} + \sum_h d_{s,h,i} - \sum_h q_h^{DAM} * (Q_{s,h,i}^{DAM,dis} - Q_{s,h,i}^{DAM,ch}) \right] \quad (59)$$

$$Z_{0,h}^{s,i} + a_{s,h,i} \geq (\pi_{\max,h}^{RTM} - \pi_{\min,h}^{RTM}) * z_{s,h,i} \quad (60)$$

$$P_{s,h,i}^{RTM,dis} - P_{s,h,i}^{RTM,ch} \leq z_{s,h,i} \quad (61)$$

$$Y_{0,h}^{s,i} + b_{s,h,i} (\pi_{\max,h}^{RTM} - \pi_{\min,h}^{RTM}) * y_{s,h,i} \quad (62)$$

$$Q_{s,h,i}^{RTM,dis} - Q_{s,h,i}^{RTM,ch} \leq y_{s,h,i} \quad (63)$$

$$W_{0,h}^{s,i} + c_{s,h,i} \geq (\pi_{\max,h}^{DAM} - \pi_{\min,h}^{DAM}) * w_{s,h,i} \quad (64)$$

$$P_{s,h,i}^{DAM,dis} - P_{s,h,i}^{DAM,ch} \leq w_{s,h,i} \quad (65)$$

$$X_{0,h}^{s,i} + d_{s,h,i} \geq (\pi_{\max,h}^{DAM} - \pi_{\min,h}^{DAM}) * x_{s,h,i} \quad (66)$$

$$Q_{s,h,i}^{DAM,dis} - Q_{s,h,i}^{DAM,ch} \leq x_{s,h,i} \quad (67)$$

$$Z_{0,h}^{s,i}, a_{s,h,i}, z_{s,h,i} \geq 0 \quad (68)$$

$$Y_{0,h}^{s,i}, b_{s,h,i}, y_{s,h,i} \geq 0 \quad (69)$$

Table 3
Parameters of BESS.

	BESS#7	BESS#15
Capacity (MWh)	10	10
Max Power Rating (MW)	10	10
Charge Efficiency	95 %	97 %
Discharge Efficiency	90 %	93 %
$\alpha_{DAM, P}$	0.16	0.14
$\beta_{DAM, Q}$	0.06	0.07
$\alpha_{RTM, P}$	0.10	0.12
$\beta_{RTM, Q}$	0.02	0.02

$$W_{0,h}^{s,i}, c_{s,h,i}, w_{s,h,i} \geq 0 \quad (70)$$

$$X_{0,h}^{s,i}, d_{s,h,i}, x_{s,h,i} \geq 0 \quad (71)$$

4. Simulation results

The IEEE 24 BUS-RTS is the test system to evaluate the efficiency of the proposed framework. Details of the system are expounded in [63]. The system has 32 generation units and one synchronous condenser (SC) at bus 14. Bus 22 has six hydro units participating in the market at a zero-bid price. Fig. 5 shows the load profile of the system. There are two BESSs owned by the private sector at bus 7 and bus 15, which are indicated by BESS#7 and BESS#15, respectively.

4.1. Deterministic clearing model of DAM and RTM

Each generator offers the active power bid to the ISO in four equal blocks. The active power bid quantity of each block is determined based on Eq. (72), and Bid # i (in Table 2) refers to offered price of i^{th} block.

Table 4

Considered contingencies to obtain APR prices in RTM.

Time	Contingency	Time	Contingency
1	Line 15–21 is out of service.	13	Loading of line 24–3 is limited to 200 MW.
2	Loading of bus 16 increases by 10 %	14	–
3	–	15	Maximum loading of line 17–18 is 200 MW.
4	Line 1–2 is out of service.	16	Generated power of hydro-units is limited to 40 MW.
5	G22 is out of service.	17	G9 is out of service.
6	Loading of bus 4 decreases by 40 %	18	Capacity of all lines connected to bus 1 is limited to 100 MW.
7	–	19	–
8	–	20	Generation of G21 and G20 are limited to 75 % of rated power.
9	Line 15–22 is out of service.	21	–
10	Loading of bus 10 decreases by 20 %	22	–
11	G3 and G4 are out of service.	23	Loading of line 19–20 is limited to 900 MW.
12	Loading of bus 2 decreases by 10 %	24	G9 is out of service.

Table 5

The results of DAM without the participation of BESS.

Time (hour)	MC _h (\$)	Q _h (MVAr)	P _h (MW)	TPF _h (\$)	Q _{pr, h} (\$/MVAr)	ρ _{P, h} (\$/MW)
1	9017.5	92.1	1541.3	309	3.35	5.65
2	9997.9	214.5	1722.2	266.9	1.24	5.65
3	9017.5	92.1	1541.3	309	3.35	5.65
4	26,148.1	316	1987.8	305.9	0.96	13
5	10,354.3	259.6	1783.8	275.6	1.06	5.65
6	9997.9	214.5	1722.2	266.9	1.24	5.65
7	27,855.2	386	2104.6	494.2	1.28	13
8	33,058.5	485.7	2511.4	409.9	0.84	13
9	34,681.3	594.3	2633.1	451	0.75	13
10	29,778.4	431	2251.6	507.3	1.17	13
11	34,687	647.3	2609.6	761.8	1.17	13
12	36,011.3	625.6	2692.5	1008.7	1.61	13
13	36,464	606.7	2719.4	1111.2	1.83	13
14	71,934.4	563.1	2963.2	520.9	0.92	24.1
15	31,539.6	378.8	2359.3	868.5	2.29	13
16	47,694	607.3	2772.6	558.6	0.91	17
17	10,354.3	259.5	1783.8	275.6	1.06	5.65
18	28,779.7	340.8	2188.3	331.6	0.97	13
19	29,778.4	431	2251.6	507.3	1.17	13
20	32,707.1	509.6	2484.4	409.1	0.80	13
21	47,694	607.3	2772.6	558.6	0.91	17
22	54,836.8	561.8	2905.8	498	0.88	18.7
23	55,400.2	529.2	2931.7	575.8	1.08	18.7
24	47,694	607.3	2772.7	558.6	0.91	17

Compared to [10], the same method (MCP) is used here with four bid levels for active power.

$$p_h^{\text{seg}, b} = \frac{P_{\max} - P_{\min}}{4} \text{ (MW)} \quad (72)$$

Table 2 displays the limits of generators and offered prices for active and reactive power. Both markets are modeled using MINLP frameworks in GAMS software and solved by SBB [64]. Moreover, the BOMINH solver is implemented to solve the robust BESS bidding/offering model. In this paper, it is assumed that the reactive power cost of BESS is paid based on the average reactive power price of DAM as indicated in Eq. (73). In Eq. (73), the TPF_h and Q_h are respectively total cost paid by ISO to all reactive power producers and total reactive power generation in *h*th period. Table 3, lists the technical data of BESSs.

Table 6

The results of RTM without the participation of BESS.

Time (Hour)	MC _h (\$)	Q _h (MVAr)	P _h (MW)	TPF _h (\$)	Q _{pr, h} (\$/MVAr)	ρ _{P, h} (\$/MW)
1	18,791.8	130.6	1545.5	245.5	1.87	12
2	10,018.2	194.7	1729.7	245.3	1.25	5.65
3	9017.5	92.08	1541.3	309	3.35	5.65
4	26,198.3	364.5	1988.7	344.5	0.94	13
5	18,218.3	155.5	1774.2	475.5	3.05	10
6	8673.4	165.2	1703	158.4	0.95	5
7	27,855.2	386	2104	494.2	1.28	13
8	33,058.5	485.7	2511	409.9	0.84	13
9	32,337.8	696.4	2642	631.4	0.90	12
10	22,656.5	486.8	2227	382.8	0.78	10
11	45,264.5	596.1	2601.6	1036.5	1.73	17
12	35,623.5	625.3	2700.6	514.6	0.82	13
13	46,602.6	569.2	2713.2	478	0.83	17
14	71,934.4	563.1	2963.2	520.9	0.92	24.1
15	31,403.7	393.4	2361	709.7	1.80	13
16	53,180.2	515.4	2762.7	1517.8	2.94	18.7
17	10,474.9	251.7	1787.2	377.1	1.49	5.65
18	32,707.1	509.6	2484.4	409.1	0.80	13
19	29,778.4	431	2251.6	507.3	1.17	13
20	32,668.9	462	2480.3	424.4	0.91	13
21	47,694	607.2	2772.6	558.6	0.91	17
22	54,836.8	561.8	2905.8	498	0.88	18.7
23	55,400.2	529.2	2931.7	575.8	1.08	18.7
24	66,773.2	429.4	2753.6	411.7	0.95	24.1

$$Q_{pr,h} = \frac{TPF_h}{Q_h} (\$/MVAr) \quad (73)$$

In the DAM, it is assumed that generators and network lines outages are not included. Table 4 presents some specific contingencies applied to the system to simulate an RTM. These contingencies for RTM are selected without using a scenario generation technique, regardless of the occurrence probability. Table 5 displays the results of the DAM settlement. Table 6 shows the results of RTM implementation. This market can present active and reactive power prices in real system conditions by applying the contingencies presented in Table 3. Fig. 6 reveals the hourly costs of DAM and RTM. Here, to examine the proposed RO bidding model for BESS, we need a set of real-time prices as inputs of the presented framework. Some random scenarios thus are generated and considered to model a typical RTM.

In Fig. 6, since generator/line failures are taken into account in the RTM, the hourly costs of RTM are generally higher than the figure for DAM. As observed in this figure, the outage of generators at hours 5, 11, 17, and 24 leads to the cost of running the market increasing significantly.

4.2. Results of robust BESS bid/offer for active and reactive power

The values required to model the PQ circle of BESS can be obtained by the trapezoidal method, as shown in Table 7.

In the following, the robust BESS bid blocks are determined in three different case studies:

Case study 1. The uncertainty budget of both markets is 100 % (Γ_{DAM} , $\Gamma_{\text{RTM}} = 100 \%$).

Case study 2. Maximization of profit of BESSs is considered. For BESS#7, this profit is achieved in the uncertainty budgets $\Gamma_{\text{DAM}} = 20 \%$ and $\Gamma_{\text{RTM}} = 80 \%$. Similarly, this goal is obtained at $\Gamma_{\text{DAM}} = 100 \%$ and $\Gamma_{\text{RTM}} = 0$ for BESS#15.

Case study 3. Minimum profit of BESSs is examined. For both BESSs, this profit is obtained in uncertainty budgets of $\Gamma_{\text{DAM}} = 10 \%$ and $\Gamma_{\text{RTM}} = 90 \%$. Table 8 shows the profit of each BESS in different conditions of DAM and RTM uncertainty budgets.

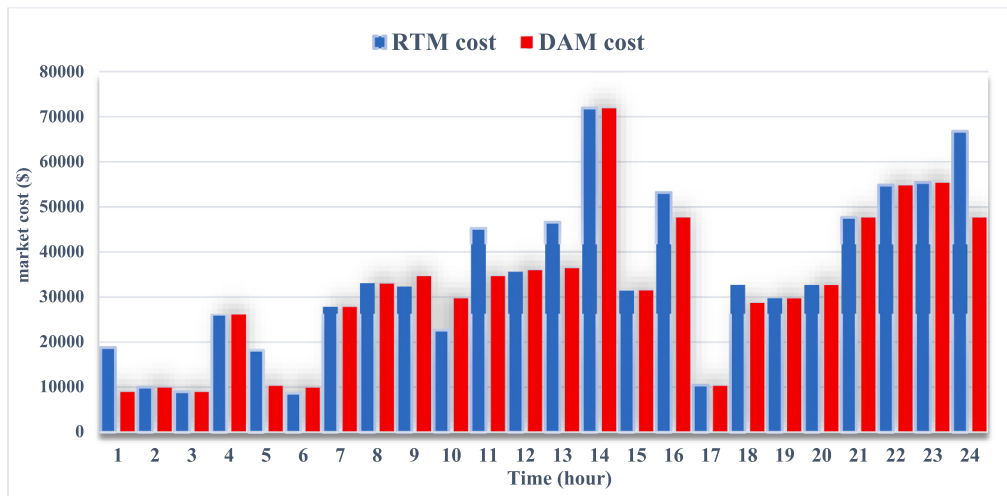


Fig. 6. Comparison of DAM and RTM costs.

Table 7
BESS modeling based on the trapezoidal method.

Tr.	$P_{n,l}$ (MW)	$P_{n,r}$ (MW)	$Q_{n,l}$ (MVar)	$Q_{n,r}$ (MVar)	M
Tr.1	-9.99	-6.66	0.447	7.46	2.106
Tr.2	-6.66	-3.33	7.46	9.43	0.6
Tr.3	-3.33	0	9.43	9.99	0.17
Tr.4	0	3.33	9.99	9.43	-0.17
Tr.5	3.33	6.66	9.43	7.46	-0.6
Tr.6	6.66	9.99	7.46	0.447	-2.106

Table 8
Profit of BESS's in different uncertainties.

Uncertainty	BESS#7 profit (\$)	BESS#15 profit (\$)		
Deterministic $\Gamma_{\text{DAM}}, \Gamma_{\text{RTM}} = 0$	808	804.46		
maximum uncertainty $\Gamma_{\text{DAM}}, \Gamma_{\text{RTM}} = 100\%$	737	764		
Sensitivity analysis $\Gamma_{\text{DAM}}, \Gamma_{\text{RTM}} = 0-100\%$	max 848.33	min 808	max 850.28	min 835.75

4.2.1. Performance of BESS #7 under various uncertainty scenarios

In the following, the bids/offers of BESS#7 in each market under three different uncertainty scenarios are represented. Figs. 7-9 show the active power dispatch scheduling of BESS#7 in three case studies. Reactive power scheduling is shown in Fig. 10 for all case studies. Fig. 11 represents SOC in the three case studies. Moreover, Fig. 12 displays the profit sensitivity of BESS #7 against the robust budget changes in each market.

Based on Fig. 7, at $t = 22$, BESS#7 sells about 90 % of its active power in DAM and 10 % in RTM. In all remaining hours, BESS#7 only participates in DAM or RTM. Due to the high price uncertainty in this case study, BESS#7 adopts a risk-averse approach and has no exchange with the market within 3 h (15, 21, 23) during the next day.

As observed from Fig. 8, at $t = 14$, BESS#7 sells about 70 % of its active power in DAM and 30 % in RTM. BESS#7 sales more active power in DAM and participates in RTM only at $t = 11, 14, 17$, and 24. In this case study, BESS#7 purchases/sells active power to maximize its profit until its operating constraints are met. Compared to case 1, to gain more profit, it exchanges energy with the network at all hours except at hour 19.

Based on Fig. 9, BESS#7 sales active power in RTM at hours 11, 17, and 24 based on higher power price rather than DAM at these hours. In case study 3, due to the owner's risk-averse policy and market price

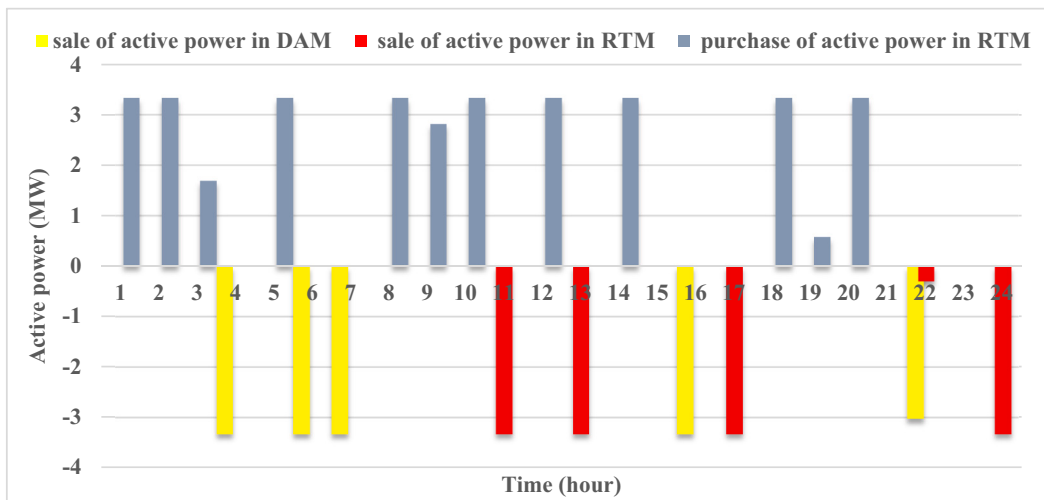


Fig. 7. Active power scheduling of BESS#7 in case study 1.

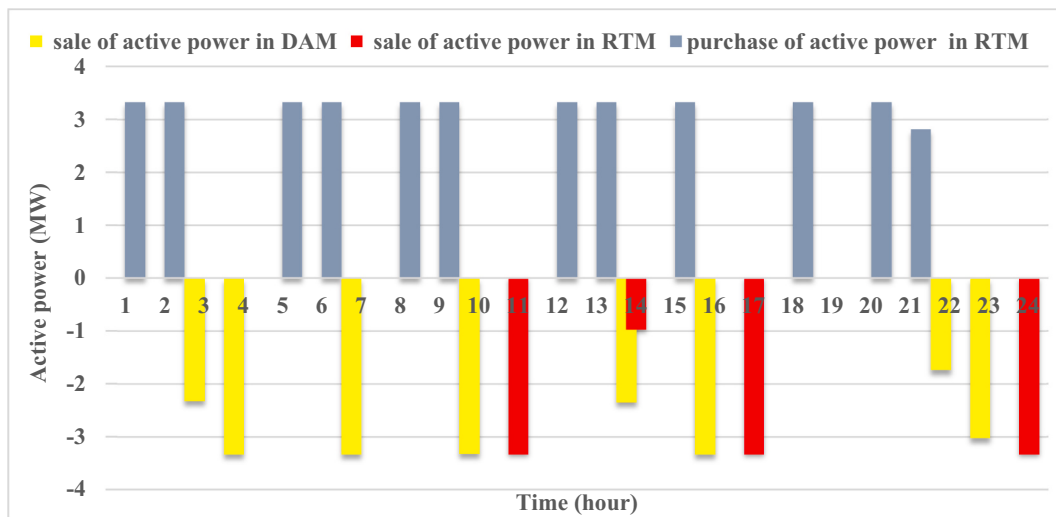


Fig. 8. Active power scheduling of BESS#7 in case study 2.

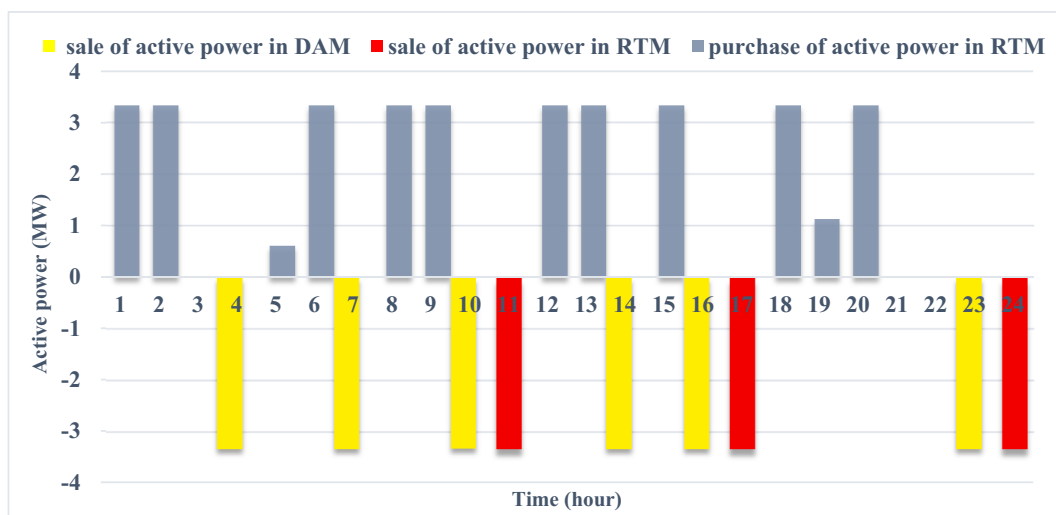


Fig. 9. Active power scheduling of BESS#7 in case study 3.

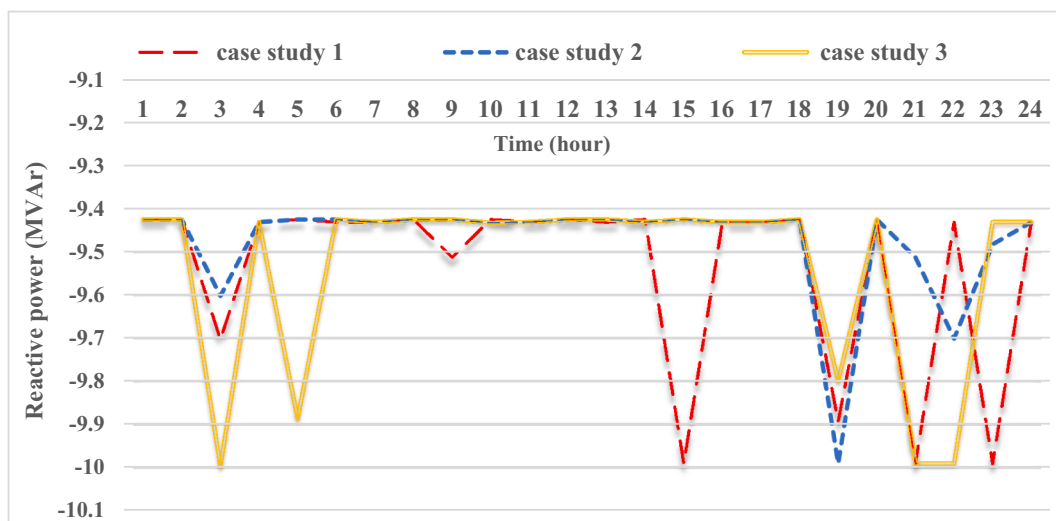


Fig. 10. Reactive power scheduling of BESS#7 in different case studies.

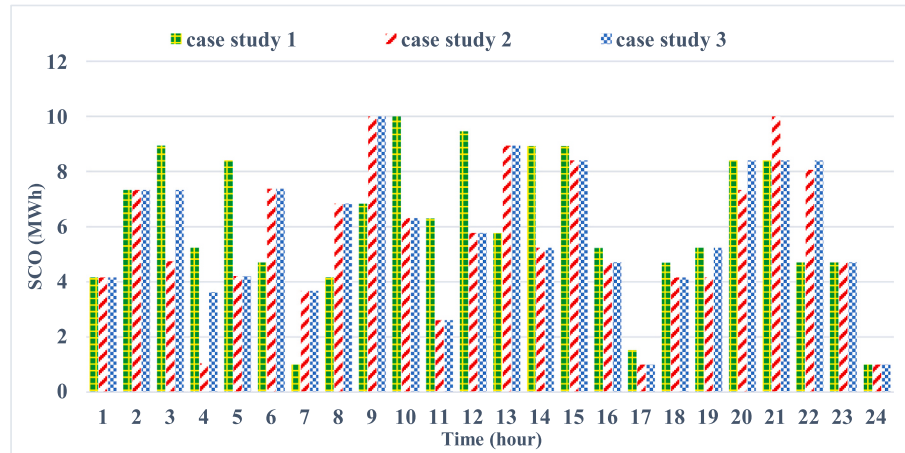


Fig. 11. SOC of BESS#7 in different case studies.

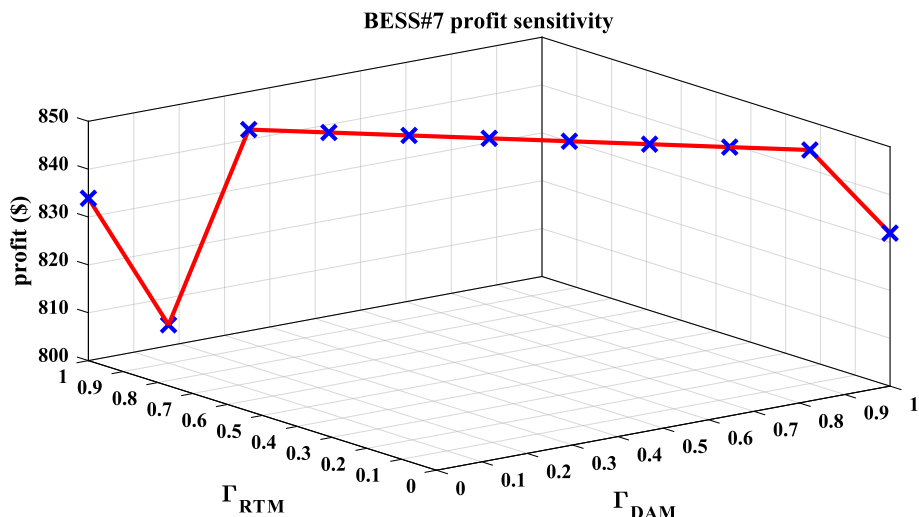


Fig. 12. profit sensitivity of BESS#7 in different scenarios based on DAM/RTM uncertainty budget.

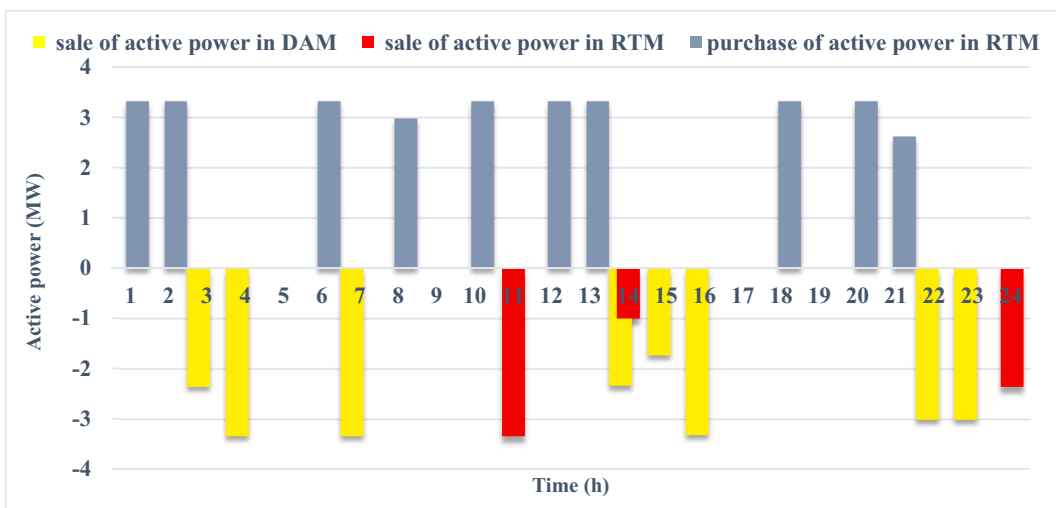


Fig. 13. Active power scheduling of BESS#15 in case study 1.

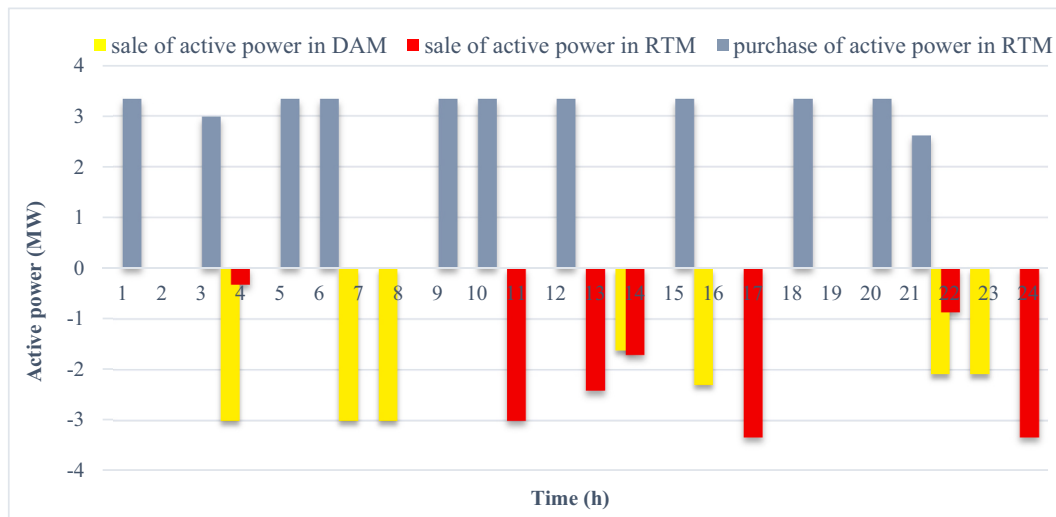


Fig. 14. Active power scheduling of BESS#15 in case study 2.

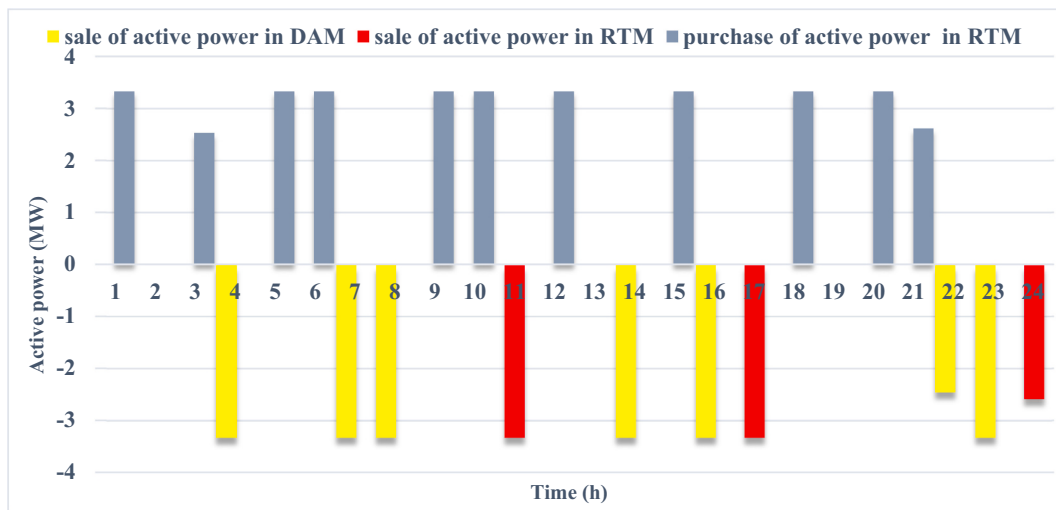


Fig. 15. Active power scheduling of BESS#15 in case study 3.

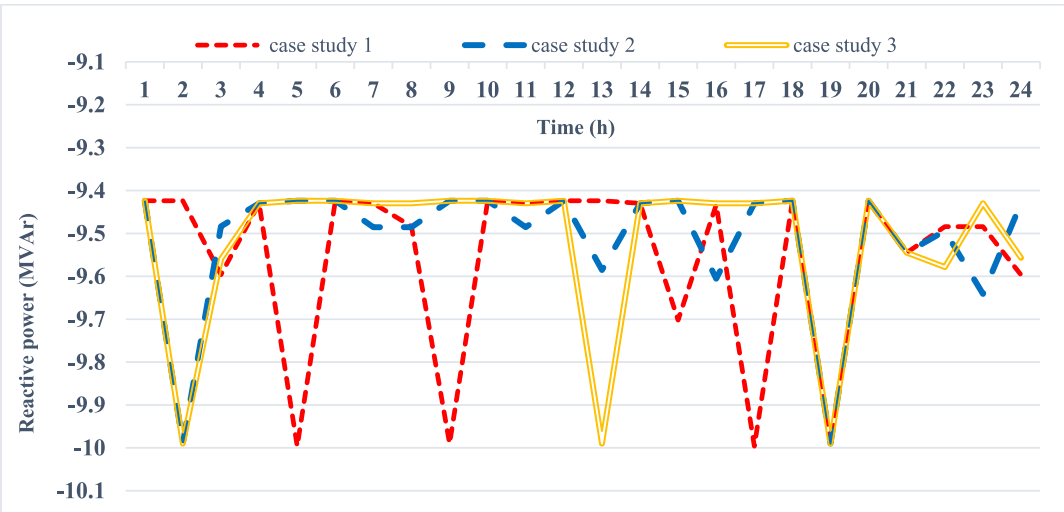


Fig. 16. Reactive power scheduling of BESS#15 in different case studies.

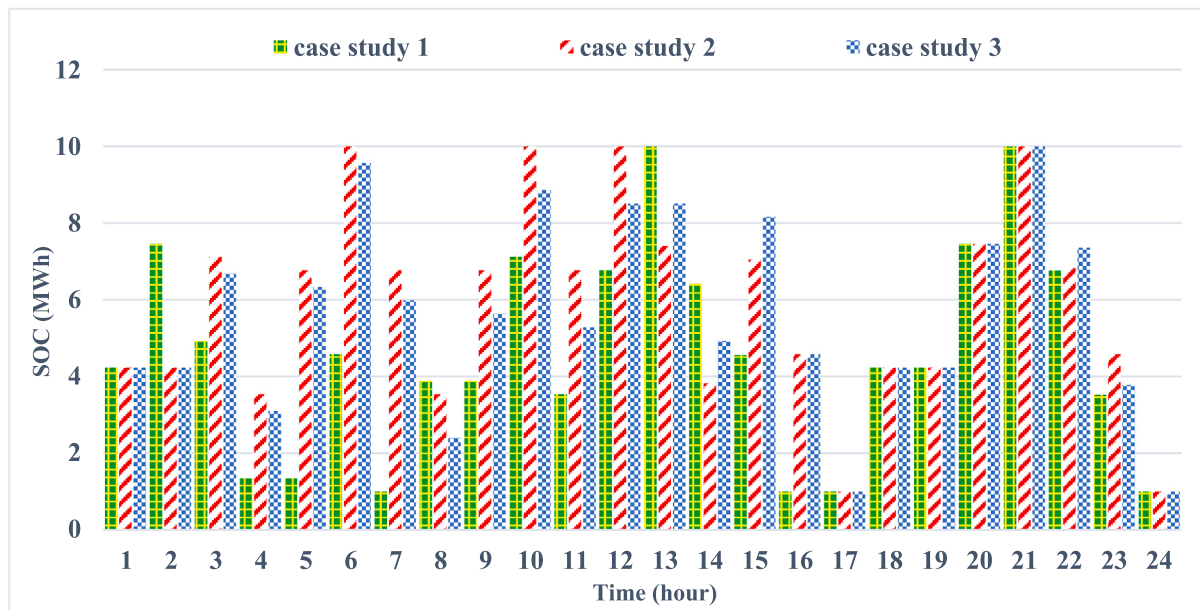


Fig. 17. SOC of BESS#15 in different case studies.

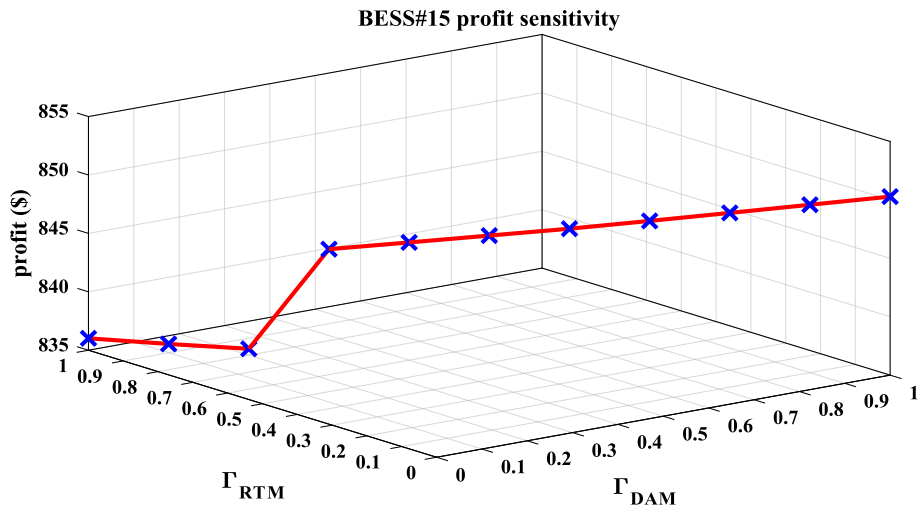


Fig. 18. Profit sensitivity of BESS#15 in different scenarios based on DAM/RTM uncertainty budget.

uncertainty conditions, at 3 h (3, 21, 22, and), no active power exchange occurs between the market and BESS#7. Therefore, the lowest profit of BESS#7 is obtained in this case.

Fig. 10 indicates the reactive power scheduling of BESS#7. As shown in Fig. 10, BESS#7 sells reactive power at all hours in the RTM. The BESS's active/reactive power dependence in the trapezoidal model enables BESS to sell a great deal of reactive power in RTM. BESS can supply nearly 10 MVar of reactive power by consuming a small amount of energy.

Fig. 11 plots the SOC of BESS#7 in different case studies. In most periods during the next day, due to the highest price uncertainty and the owner's risk aversion policy, case study 1 has the highest SOC. According to Eq. (25), in the last hour of scheduling, all three cases have the same SOC, i.e., 1MWh.

As shown in Fig. 12, the variations of BESS#7 profit are obtained by changing the budget uncertainty of both the DA and RT markets. According to the simulation results illustrated in Fig. 12, the highest and lowest profits of the owner of BESS#7 are acquired in $\Gamma_{\text{DAM}} = 20\%$, $\Gamma_{\text{RTM}} = 80\%$ and $\Gamma_{\text{DAM}} = 10\%$, $\Gamma_{\text{RTM}} = 90\%$, respectively.

4.2.2. Performance of BESS#15 in different uncertainty scenarios

Here, the bids/offers of BESS#15 in each market under three different uncertainty scenarios are represented. Figs. 13–15 describe the active power dispatching of BESS#15 in the three case studies. Fig. 16 displays the reactive power scheduling of BESS#15. Fig. 16 shows that BESS#15 sells reactive power at all RTM periods, similar to BESS#7. Fig. 17 represents SOC in the three case studies. Moreover, Fig. 18 displays the profit sensitivity of BESS#15 against the robust budget changes in each market.

As shown in Fig. 13, at hour 14, BESS #15 sells 69 % of active power in the DAM and 31 % in the RTM. In this case study, due to considering maximum uncertainty, BESS has no active power transactions with the market at 4 h, 5, 9, 17, and 19.

It is displayed in Fig. 14, at $t = 4$, BESS#15 sells 90 % of active power in the DAM and 10 % in the RTM; at $t = 14$, it sells 48 % of active power in the DAM and 52 % in the RTM, and at $t = 22$, it sells 62 % of active power in the DAM and 38 % in the RTM. In this case, simultaneous participation of BESS in 3 h of DAM and RTM occurs only to obtain maximum profit.

Table 9BESS effect on DAM settlement in [case study 1](#) (worst case).

Time (hour)	ISO surplus (\$)	Loss (MW)	MC_h (\$)	Q_h (MVAr)	P_h (MW)	TPF_h (\$)	$Q_{pr, h}$ (\$/MVAr)	$\rho_{P, h}$ (\$/MW)
1	6622	30.8	9017	92	1541.3	309	3.35	5.65
2	6958	40.7	9997	214.5	1722.2	266.9	1.24	5.65
3	6558.1	28.3	9033	88.4	1540.5	329.6	3.72	5.65
4	19,503	35.7	25,926	256.2	1975.9	238.3	0.92	13
5	6960	45.3	10,354	259.5	1783.8	275.6	1.06	5.65
6	5754	37.5	8943	210.5	1721	338	1.60	5
7	18,255	48.5	25,550	399	2102.9	315.4	0.79	12
8	19,636	60.4	33,058	485.7	2511.4	409.9	0.84	13
9	19,867	68.1	34,681	594.3	2633.1	451	0.75	13
10	20,354	57.1	29,778	431	2251.6	507.3	1.17	13
11	19,801	73.1	34,687	647.3	2609.6	761.8	1.17	13
12	19,059	70.5	36,011	625.5	2692.5	1008.7	1.61	13
13	20,272	68.9	36,464	606.7	2719.4	1111.2	1.83	13
14	48,379	53.7	71,925	552.3	2964.1	490.35	0.88	24.1
15	15,121	66.4	26,808	567.1	2377.6	654.1	1.15	11
16	30,442	55.2	47,693	562.3	2765.9	672.4	1.19	17
17	6959	45.3	10,354	259.5	1783.8	275.6	1.06	5.65
18	19,028	50.8	28,779	340.8	2188.3	331.6	0.97	13
19	20,354	57.1	29,778	431	2251.6	507.3	1.17	13
20	20,307	61.9	32,707	509.6	2484.4	409.1	0.80	13
21	30,489	65.1	47,694	607.2	2772.6	558.6	0.91	17
22	33,593	49.1	54,761	546.1	2902.4	485.1	0.88	18.7
23	33,673	52.6	55,362	549.4	2934.4	487.7	0.88	18.7
24	30,489	65.1	47,694	607.2	2772.6	558.6	0.91	17

Table 10BESS effect on DAM settlement in [case study 2](#) (maximum profit).

Time (hour)	ISO surplus (\$)	Loss (MW)	MC_h (\$)	Q_h (MVAr)	P_h (MW)	TPF_h (\$)	$Q_{pr, h}$ (\$/MVAr)	$\rho_{P, h}$ (\$/MW)
1	6622.2	30.8	9017.5	92	1541.3	309	3.35	5.65
2	6958.4	40.7	9997.9	214.5	1722.2	267	1.24	5.65
3	5814.5	28.1	9032.3	87.8	1540.4	328.7	3.74	5.65
4	19,736	38.6	26,073	279.1	1978.9	347.8	1.24	13
5	6959.9	45.3	10,354	259.5	1783.8	275.6	1.06	5.65
6	6958.4	40.7	9997.9	214.5	1722.2	266.9	1.24	5.65
7	17,825	48.8	25,554	399	2103.2	315.4	0.79	12
8	19,336	55.3	33,043	456.8	2509.1	423.8	0.92	13
9	19,867	68.1	34,681	594.2	2633.1	451	0.75	13
10	18,571	51.4	29,585	415.9	2248.4	354.8	0.85	13
11	19,801	73.1	34,687	647.2	2609.6	761.8	1.17	13
12	19,059	70.5	36,011	625.5	2692.5	1008.7	1.61	13
13	20,272	68.9	36,464	606.7	2719.4	1111.6	1.83	13
14	48,618	52.1	71,907	551.5	2962.5	511.4	0.92	24.1
15	19,715	50.8	31,539	378.8	2359.3	868.5	2.29	13
16	30,450	57.8	47,485	587.3	2768.4	421.4	0.71	17
17	6959.9	45.3	10,354	259.5	1783.8	275.6	1.06	5.65
18	19,028	50.8	28,779	340.8	2188.3	331.6	0.97	13
19	20,354	57.1	29,778	431	2251.6	507.3	1.17	13
20	20,307	61.9	32,707	509.6	2484.4	409.1	0.80	13
21	30,489	65.1	47,694	607.2	2772.6	558.6	0.91	17
22	34,655	51.7	54,771	549.5	2905	447.1	0.81	18.7
23	33,377	50.4	55,279.11	547.7	2932.2	445.7	0.81	18.7
24	30,489	65.1	47,694	607.2	2772.6	558.6	0.91	17

As can be seen from [Fig. 15](#), in [case study 3](#) which minimum profit for BESS#15 is obtained, no active power exchange occurs within 3 h (2, 13, 19, and) in the DAM and RTM.

[Fig. 16](#) shows BESS#15 optimal reactive power scheduling. During hours with the lowest active power exchange, BESS#15 can sell the maximum possible reactive power, i.e., about 10 MVAr, in the market. Since the exchange of active power in DAM maximizes the profit of BESS, in all three cases, the discharge of reactive power is accomplished only in the RTM for both BESSs.

As observed in [Fig. 17](#), owing to the robust policy and different efficiencies, the SOC of BESS#15 changes generally differs from BESS#7. From hours 3 to 13, the SOC of [case study 2](#) is higher than that of case studies 1 and 3. While after hour 17, all three case studies have the same SOC.

The profit of BESS#15 vs. the DAM and RTM uncertainty budget variations is shown in [Fig. 18](#). Unlike BESS#7, BESS#15 profit is inversely related to the variations of the DAM uncertainty budget (Γ_{DAM}). From 100 % to 70 % of Γ_{DAM} (or up to 30 % of Γ_{RTM}), the profit is almost constant, and from 70 % to 0 of Γ_{DAM} (or from 30 % to 100 % of Γ_{RTM}), the profit has increased significantly. The highest profit of BESS#15 is achieved in $\Gamma_{DAM} = 100$ % and $\Gamma_{RTM} = 0$ %. Similar to BESS#7, the lowest profit of BESS#15 is also obtained in $\Gamma_{DAM} = 10$ % and $\Gamma_{RTM} = 90$ %. Given the participation of both BESSs in three case studies, the market settlement results are displayed in [Tables 9, 10, and 11](#), respectively. The results include market costs and the price and production of active and reactive power. [Table 12](#) summarizes the simulation results of the three case studies. [Table 12](#) summarize the result of BESS's participation. The main effects of BESS are related to the

Table 11BESS effect on DAM settlement in [case study 3](#) (minimum profit).

Time (hour)	ISO surplus (\$)	Loss (MW)	MC_h (\$)	Q_h (MVAr)	P_h (MW)	TPF_h (\$)	$Q_{pr, h}$ (\$/MVAr)	$\rho_{P, h}$ (\$/MW)
1	6622	30.8	9017.5	92	1541.3	309	3.35	5.65
2	6958	40.7	9997.9	214.5	1722.2	266	1.24	5.65
3	6622	30.8	9017.5	92	1541.3	309	3.35	5.65
4	19,503	35.7	25,926	256.2	1975.9	238	0.92	13
5	6959	45.3	10,354	259.5	1783.8	275	1.06	5.65
6	6958	40.7	9997.9	214.5	1722.2	266	1.24	5.65
7	18,255	48.5	25,550	399	2102.9	315	0.79	12
8	19,636	60.4	33,058	485.7	2511.4	409	0.84	13
9	19,867	68.1	34,681	594.3	2633.1	451	0.75	13
10	18,571	51.4	29,585	415.9	2248.4	354	0.85	13
11	19,801	73.1	34,687	647.3	2609.6	761	1.17	13
12	19,059	70.5	36,011	625.5	2692.5	1008	1.61	13
13	20,272	68.9	36,464	606.7	2719.4	1111	1.83	13
14	45,352	49.4	68,587	551.4	2959.8	511	0.92	23
15	19,715	50.8	31,539	378.8	2359.3	868	2.29	13
16	29,969	56.4	47,552	586	2767	512	0.87	17
17	6959	45.3	10,354	259.5	1783	275	1.06	5.65
18	19,028	50.8	28,779	340.8	2188	331	0.97	13
19	20,354	57.1	29,778	431	2251.6	507	1.17	13
20	20,307	61.9	32,707	509.6	2484.4	409	0.80	13
21	30,489	65.1	47,694	607.2	2772.6	558	0.91	17
22	34,671	52.4	54,923	482.9	2905.7	585	1.21	18.7
23	33,849	49.1	55,261	552.6	2931	452	0.81	18.7
24	30,489	65.1	47,694	607.2	2772.6	558	0.91	17

Table 12

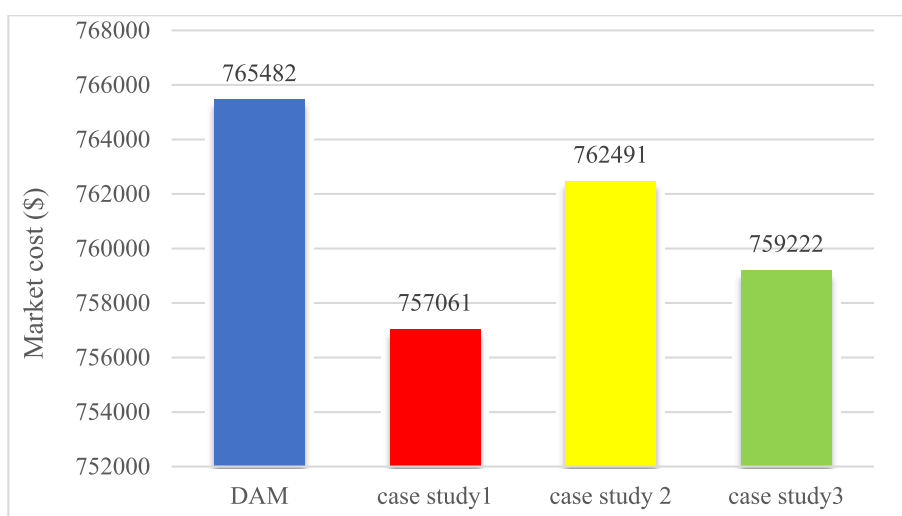
Summary of technical and economic effects of BESS in different case studies.

	DAM without BESS	Case study 1	Case study 2	Case study 3
Market cost (\$)	765,842	757,061	762,491	759,222
Total Active power (MW)	56,007	56,003.81	55,985.87	55,981
Total Reactive power (MVAr)	10,361	10,444	10,264	10,211
Average active power price (\$/MW)	12.6	12.44	12.55	12.51
Average reactive power price (\$/MVAr)	1.32	1.29	1.30	1.29
Loss (MW)	1316	19,1288	1269.48	1269.311
BESS profit (\$)	–	1501	1698	1613
ISO Surplus (\$)	–	6920	1293	4616

reduction in the market cost compared to the basic DAM model without BESS. [Figs. 19-22](#) indicate BESS's economic and technical impact on the system.

In the proposed trapezoidal model indicated in [Fig. 4](#), due to active and reactive power prices, BESS bids in all market periods are expressed in the lower part of trapezoids 3 and 4, i.e., the maximum reactive power sales at the boundary points of the curve (at maximum active power). Considering the participation of BESSs in all three case studies, the market's overall cost decreases compared to the base case, as shown in [Fig. 19](#). [Case study 1](#) outperforms other case studies in reducing the overall market cost (6920 \$). The minimum market cost reduction is related to [case study 2](#). This result stems from the conflict of interest between BESS and ISO.

To evaluate the positive impact of BESS participation in the active and reactive power prices, a new performance index as the average active and reactive power price is introduced by dividing total prices during a day by 24, as shown in [Fig. 20](#). As shown in [Fig. 20](#), the average prices of active and reactive power have decreased in all three case

**Fig. 19.** Market cost comparison in different case studies.

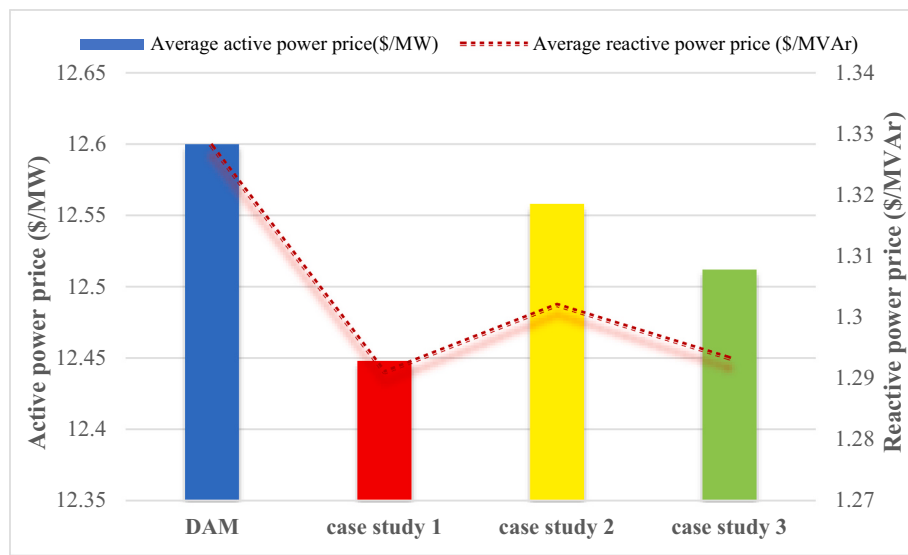


Fig. 20. Average active and reactive power prices in different case studies.

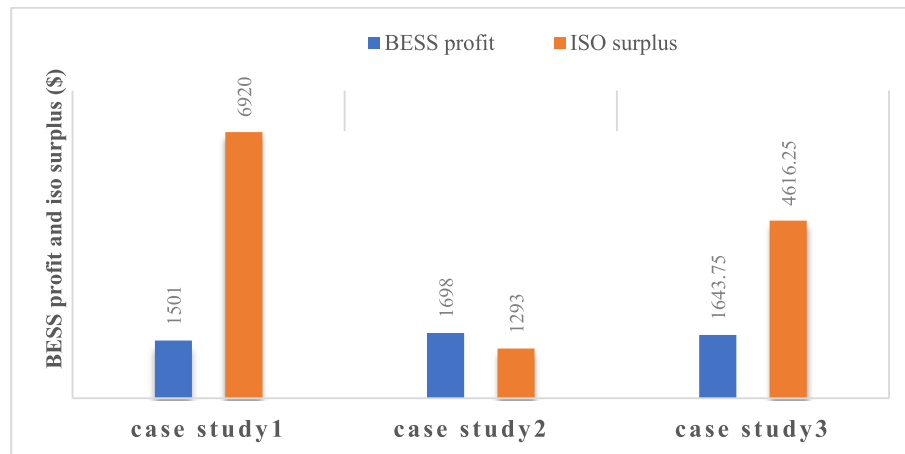


Fig. 21. Effect of BESS in different case studies.

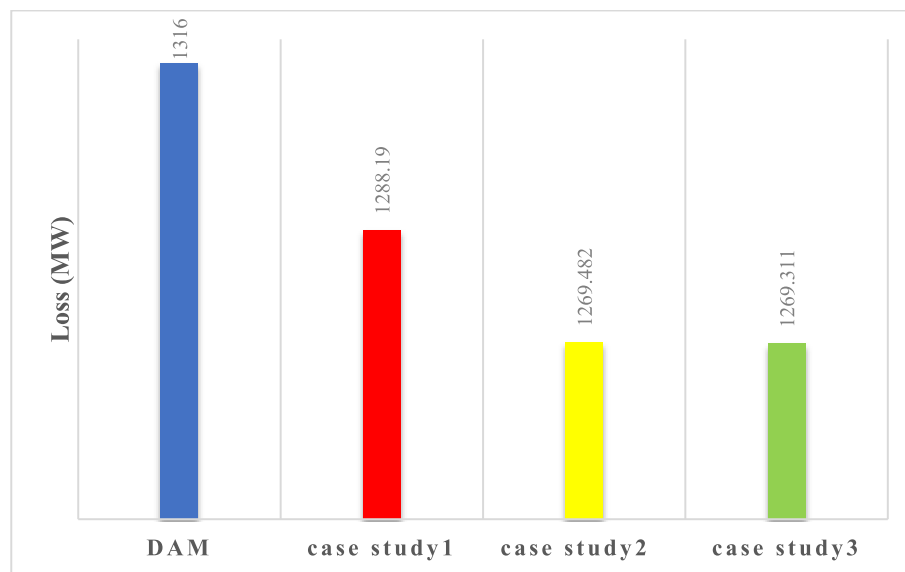


Fig. 22. BESS effect on active power losses in three case studies.

studies with BESS. The highest decrease in the average prices of active power and reactive power, respectively 2 % and 3 %, is related to [case study 1](#).

Based on [Fig. 21](#), from the ISO viewpoint, the best performance of BESS on ISO surplus can be achieved in [case study 1](#). Whereas the best performance of BESS on its private owner's profit is in [case study 2](#), which is the only case in which the profit of the private owner of BESS is more than the ISO surplus. Nevertheless, since the BESSs aim to maximize their profits, [case study 2](#) contributes to the highest profit and optimal operation mode.

The positive impact of BESS in reducing network real losses is observed in [Fig. 22](#). As shown, system losses in all three cases have decreased compared to the primary DAM (without BESS). The first case study leads to a 2 % decrease in losses, while a 3.5 % decrease in losses occurs in case studies 2 and 3.

5. Conclusion

In this paper, an active and reactive power robust bid/offer framework has been modeled for private-sector owners of BESS using the trapezoidal method. The deterministic model of the JARPM on DAM and RTM time horizon the primary prices to provide the basis for setting up a private-sector owned robust bid/offer BESS model. A robust counterpart and the duality theory were employed to solve the proposed RO model. Next, regarding the worst uncertainty conditions and the owner's adoption of two different approaches, the DAM market was implemented considering the BESS bid blocks in GAMS on the system test IEEE24-RTS system. Finally, the proposed model's efficiency was proved through the reduction of costs and losses for the ISO and the profit of BESSs. The simulation results briefly show that:

In the worst uncertainty condition ([case study 1](#)), participation of BESSs would reduce the market cost by 6920 \$ within a 24-h. Due to the conflict of interests between BESS and ISO as two profit-oriented market players, the BESS owner's maximum profit, achieved in [case study 2](#), leads to a minimum ISO surplus. The participation of BESSs in the maximum uncertainty ([case study 1](#)) contributes to the highest decrease in the average price of active power. On the other hand, as indicated in [case study 2](#), BESS's transactions to maximize their profits lead to the lowest reduction in the average active and reactive power prices compared to other case studies. BESS's participation in all three case studies reduces real power system losses. Although the capacity of installed BESSs is 0.7 % of the total system load, it contributes to a 2 %-3.5 % reduction in real power losses. The simulation results show that the average price of active and reactive power is reduced by 2 % and 3 %, respectively, and the overall cost of running DAM is reduced between 68 and 288 \$/hour. On the other hand, the robust framework proposed in the three case studies also guarantees a reasonable profit level (30–35 \$/hour) for the private owner. In future works, the presented model can be extended by incorporating DR programs and load-price sensitivity along with high penetration of RES as either a single-objective or multi-objective optimization problem.

CRediT authorship contribution statement

Mohammad Farahani: Investigation, Methodology, Data curation, Software, Visualization.

Abouzar Samimi: Conceptualization, Writing- Original draft preparation, Supervision, Validation.

Hossein Shateri: Resources, Writing- Reviewing and Editing, Validation.

Declaration of competing interest

The authors declare that they have no known competing financial interests or personal relationships that could have appeared to influence the work reported in this paper.

Data availability

Data will be made available on request.

References

- [1] M.L. Baughman, S.N. Siddiqi, Real-time pricing of reactive power: theory and case study results, *IEEE Trans. Power Syst.* (1991), <https://doi.org/10.1109/59.131043>.
- [2] J. Zhong, K. Bhattacharya, Toward a competitive market for reactive power, *IEEE Trans. Power Syst.* (2002), <https://doi.org/10.1109/TPWRS.2002.805025>.
- [3] J. Zhong, E. Nobile, A. Bose, K. Bhattacharya, Localized reactive power markets using the concept of voltage control areas, *IEEE Trans. Power Syst.* 19 (3) (2004) 1555–1561, <https://doi.org/10.1109/TPWRS.2004.831656>.
- [4] A. Ketabi, A. Alibabaei, R. Feuillet, Application of the ant colony search algorithm to reactive power pricing in an open electricity market, *Int. J. Electr. Power Energy Syst.* 32 (6) (2010) 622–628, <https://doi.org/10.1016/j.ijepes.2009.11.019>.
- [5] N.R. Ullah, K. Bhattacharya, T. Thiringer, Wind farms as reactive power ancillary service providers-technical and economic issues, *IEEE Trans. Energy Convers.* 24 (3) (2009) 661–672, <https://doi.org/10.1109/TEC.2008.2008957>.
- [6] M. Mir, M. Shafieezadeh, M.A. Heidari, N. Ghadimi, Application of hybrid forecast engine based intelligent algorithm and feature selection for wind signal prediction, *Evol. Syst.* 11 (4) (2020) 559–573, <https://doi.org/10.1007/s12530-019-09271-y>.
- [7] P. Akbary, M. Ghiasi, M.R.R. Pourkheranjani, H. Alipour, N. Ghadimi, Extracting appropriate nodal marginal prices for all types of committed reserve, *Comput. Econ.* 53 (1) (2019) 1–26, <https://doi.org/10.1007/s10614-017-9716-2>.
- [8] M. Yebiyo, R.A. Mercado, A. Gillich, I. Chaer, A.R. Day, A. Paurine, Novel economic modelling of a peer-to-peer electricity market with the inclusion of distributed energy storage—the possible case of a more robust and better electricity grid, *Electr. J.* 33 (2) (2020), 106709, <https://doi.org/10.1016/j.tej.2020.106709>.
- [9] H. Ahmadi, A. Akbari Foroud, A stochastic framework for reactive power procurement market, based on nodal price model, *Int. J. Electr. Power Energy Syst.* 49 (1) (2013) 104–113, <https://doi.org/10.1016/j.ijepes.2012.12.013>.
- [10] A. Azadeh, M.R. Skandari, B. Maleki-Shoja, An integrated ant colony optimization approach to compare strategies of clearing market in electricity markets: agent-based simulation, *Energy Policy* 38 (10) (2010) 6307–6319, <https://doi.org/10.1016/j.enpol.2010.06.022>.
- [11] A. Samimi, M. Nikzad, Complete active-reactive power resource scheduling of smart distribution system with high penetration of distributed energy resources, *J. Mod. Power Syst. Clean Energy* 5 (6) (2017) 863–875, <https://doi.org/10.1007/s40565-017-0330-z>.
- [12] A. Samimi, M. Nikzad, A. Kazemi, Coupled active and reactive market in smart distribution system considering renewable distributed energy resources and demand response programs, *Int. Trans. Electr. Energy Syst.* 27 (4) (2017) 1–18, <https://doi.org/10.1002/etep.2268>.
- [13] A. Samimi, Probabilistic day-ahead simultaneous active/reactive power management in active distribution systems, *J. Mod. Power Syst. Clean Energy* 7 (6) (2019) 1596–1607, <https://doi.org/10.1007/s40565-019-0535-4>.
- [14] T. Ishizaki, M. Koike, N. Yamaguchi, Y. Ueda, J. Imura, Day-ahead energy market as adjustable robust optimization: spatio-temporal pricing of dispatchable generators, storage batteries, and uncertain renewable resources, *Energy Econ.* 91 (2020), 104912, <https://doi.org/10.1016/j.eneco.2020.104912>.
- [15] D. Jay, K.S. Swarup, A comprehensive survey on reactive power ancillary service markets 144, 2021 no. September 2020.
- [16] K. Jain, M.B. Jasser, M. Hamzah, A. Saxena, A.W. Mohamed, Harris hawk optimization-based deep neural networks architecture for optimal bidding in the electricity market, *Mathematics* 10 (12) (2022) 1–19, <https://doi.org/10.3390/math10122094>.
- [17] M. Nazari-Heris, B. Mohammadi-Ivatloo, Application of Robust Optimization Method to Power System Problems, Elsevier Inc., 2018, <https://doi.org/10.1016/B978-0-12-812441-3.00002-1>.
- [18] A.L. Soyster, Convex programming with set-inclusive constraints and applications to inexact linear programming, *Oper. Res.* 21 (5) (2016) 1154–1157 [Online]. Available: <https://www.jstor.org/stable/pdf/168933.pdf?refreqid=excelsior%3A8ef7d3bc8ba28376c4b0b37fb411d07>.
- [19] M.R. AkbariZadeh, T. Niknam, A. Kavousi-Fard, Adaptive robust optimization for the energy management of the grid-connected energy hubs based on hybrid meta-heuristic algorithm, *Energy* 235 (Nov. 2021), 121171, <https://doi.org/10.1016/J.ENERGY.2021.121171>.
- [20] X. Zhu, J. Wu, D. Liu, Robust unit commitment for minimizing wind spillage and load shedding with optimal DPFC, *Front. Energy Res.* 10 (April) (2022) 1–13, <https://doi.org/10.3389/fenrg.2022.877042>.
- [21] V.A.F. De Campos, J.J. Da Cruz, L.C. Zanetta, Robust and optimal adjustment of power system stabilizers through linear matrix inequalities, *Int. J. Electr. Power Energy Syst.* 42 (1) (Nov. 2012) 478–486, <https://doi.org/10.1016/J.IJEPES.2012.04.025>.
- [22] C. Chen, Y.P. Li, G.H. Huang, Y.F. Li, in: Electrical power and energy systems a robust optimization method for planning regional-scale electric power systems and managing carbon dioxide 40, 2012, pp. 70–84, <https://doi.org/10.1016/J.IJEPES.2012.02.007>.
- [23] S.A. Mansouri, M.S. Javadi, A robust optimisation framework in composite generation and transmission expansion planning considering inherent uncertainties, *J. Exp. Theor. Artif. Intell.* 29 (4) (2017) 717–730, <https://doi.org/10.1080/0952813X.2016.1259262>.

- [24] M.S. Javadi, A. Anvari-Moghaddam, J.M. Guerrero, Robust energy hub management using information gap decision theory, in: Proc. IECON 2017 - 43rd Annu. Conf. IEEE Ind. Electron. Soc vol. 2017-Janua, 2017, pp. 410–415, <https://doi.org/10.1109/IECON.2017.8216073>.
- [25] A.R. Jordehi, M.S. Javadi, M. Shafie-khah, J.P.S. Catalão, Information gap decision theory (IGDT)-based robust scheduling of combined cooling, heat and power energy hubs, Energy 231 (2021), <https://doi.org/10.1016/j.energy.2021.120918>.
- [26] M.H. Shams, M. Mansourlakouraj, M. Shahabi, M.S. Javadi, J.P.S. Catalao, Robust scenario-based approach for the optimal scheduling of energy hubs, in: 2021 IEEE Madrid PowerTech, PowerTech 2021 - Conf. Proc vol. 029803, 2021, pp. 3–8, <https://doi.org/10.1109/PowerTech46648.2021.9494837>.
- [27] S.A. Mansouri, E. Nematabkhsh, A. Ahmarnajad, A.R. Jordehi, M.S. Javadi, S.A. A. Matin, A multi-objective dynamic framework for design of energy hub by considering energy storage system, power-to-gas technology and integrated demand response program, J. Energy Storage 50 (Jun. 2022), 104206, <https://doi.org/10.1016/J.est.2022.104206>.
- [28] A. H. Hajimiragha C. A. Ca M. W. Fowler S. Moaveni A. Elkamel M. Carlo , “A Robust Optimization Approach for Planning the Transition to Plug-in Hybrid Electric Vehicles,” pp. 1–11.
- [29] A. Andreotti, G. Carpinelli, F. Mottola, D. Proto, A. Russo, Decision theory criteria for the planning of distributed energy storage systems in the presence of uncertainties, IEEE Access 6 (2018) 62136–62151, <https://doi.org/10.1109/ACCESS.2018.2876236>.
- [30] J. Liu, C. Chen, Z. Liu, K. Jermitsittiparsert, N. Ghadimi, An IGDT-based risk-optimal bidding strategy for hydrogen storage-based intelligent parking lot of electric vehicles, J. Energy Storage 27 (August 2019) (2020) 101057, <https://doi.org/10.1016/j.est.2019.101057>.
- [31] M. Vahid-Ghavidel, et al., Novel hybrid stochastic-robust optimal trading strategy for a demand response aggregator in the wholesale electricity market, IEEE Trans. Ind. Appl. 57 (5) (2021) 5488–5498, <https://doi.org/10.1109/TIA.2021.3098500>.
- [32] Z. Wang, A. Negash, D.S. Kirschen, Optimal scheduling of energy storage under forecast uncertainties, IET Gener. Transm. Distrib. 11 (17) (2017) 4220–4226, <https://doi.org/10.1049/iet-gtd.2017.0037>.
- [33] M. Zugno, A.J. Conejo, A robust optimization approach to energy and reserve dispatch in electricity markets, Eur. J. Oper. Res. 247 (2) (2015) 659–671, <https://doi.org/10.1016/j.ejor.2015.05.081>.
- [34] A. Akbari-dibavar, K. Zare, S. Nojavan, A hybrid stochastic-robust optimization approach for energy storage arbitrage in day-ahead and real-time markets, Sustain. Cities Soc. (2019), 101600, <https://doi.org/10.1016/j.scs.2019.101600>.
- [35] A. Soroudi, Robust optimization based self scheduling of hydro-thermal genco in smart grids, Energy 61 (2013) 262–271, <https://doi.org/10.1016/j.energy.2013.09.014>.
- [36] A.J. Conejo, X. Wu, Robust optimization in power systems: a tutorial overview, Optim. Eng. (0123456789) (2021), <https://doi.org/10.1007/s11081-021-09667-3>.
- [37] H. Mehrjerdi, R. Hemmati, E. Farrokhi, Nonlinear stochastic modeling for optimal dispatch of distributed energy resources in active distribution grids including reactive power, Simul. Model. Pract. Theory 94 (October 2018) (2019) 1–13, <https://doi.org/10.1016/j.simpat.2019.01.005>.
- [38] A. Barbry, M.F. Anjos, E. Delage, K.R. Schell, Robust self-scheduling of a price-maker energy storage facility in the New York electricity market, Energy Econ. 78 (2019) (2019) 629–646, <https://doi.org/10.1016/j.eneco.2018.11.003>.
- [39] M. Kazemi, H. Zareipour, N. Amjadi, W.D. Rosehart, M. Ehsan, Operation scheduling of battery storage systems in joint energy and ancillary services markets, IEEE Trans. Sustain. Energy 8 (4) (2017) 1726–1735, <https://doi.org/10.1109/TSTE.2017.2706563>.
- [40] D. Krishnamurthy, C. Uckun, Z. Zhou, P.R. Thimmapuram, A. Botterud, Energy storage arbitrage under day-ahead and real-time price uncertainty, IEEE Trans. Power Syst. 33 (1) (2017) 84–93, <https://doi.org/10.1109/tpwrs.2017.2685347>.
- [41] H. Mohsenian-Rad, Coordinated price-maker operation of large energy storage units in nodal energy markets, IEEE Trans. Power Syst. 31 (1) (2016) 786–797, <https://doi.org/10.1109/TPWRS.2015.2411556>.
- [42] M.S. Javadi, K. Firuzi, M. Rezanejad, M. Lotfi, M. Gough, J.P.S. Catalao, Optimal sizing and siting of electrical energy storage devices for smart grids considering time-of-use programs, in: IECON Proc. (Industrial Electron. Conf vol. 2019-Octob, 2019, pp. 4157–4162, <https://doi.org/10.1109/IECON.2019.8927263>.
- [43] W. Cai, R. Mohammadtab, G. Fathi, K. Wakil, A.G. Ebadi, N. Ghadimi, Optimal bidding and offering strategies of compressed air energy storage: a hybrid robust stochastic approach, Renew. Energy 143 (2019) 1–8, <https://doi.org/10.1016/j.renene.2019.05.008>.
- [45] F. Mirzapour, M. Lakzaei, G. Varamini, M. Teimourian, N. Ghadimi, A new prediction model of battery and wind-solar output in hybrid power system, J. Ambient. Intell. Humaniz. Comput. 10 (1) (2019) 77–87, <https://doi.org/10.1007/s12652-017-0600-7>.
- [46] S.A. Mansouri, E. Nematabkhsh, M.S. Javadi, A.R. Jordehi, M. Shafie-khah, J.P. S. Catalão, Resilience enhancement via automatic switching considering direct load control program and energy storage systems no. 3 EEEIC/I&CPS Eur 1, 2021, pp. 1–6, <https://doi.org/10.1109/EEEIC/I&CPS Eur 1.2021.9584609>.
- [47] Z. Yang, et al., Robust multi-objective optimal design of islanded hybrid system with renewable and diesel sources/stationary and mobile energy storage systems, Renew. Sust. Energ. Rev. 148 (Sep. 2021), 111295, <https://doi.org/10.1016/j.rser.2021.111295>.
- [48] H. Khani, et al., Joint arbitrage and operating reserve scheduling of energy storage through optimal adaptive allocation of the state of charge, IEEE Trans. Sustain. Energy 7 (1) (2016) 5115–5124, <https://doi.org/10.1109/TPWRS.2017.2705187>.
- [49] G. He, Q. Chen, C. Kang, P. Pinson, Q. Xia, Optimal bidding strategy of battery storage in power markets considering performance-based regulation and battery cycle life, IEEE Trans. Smart Grid 7 (5) (2016) 2359–2367, <https://doi.org/10.1109/TSG.2015.2424314>.
- [50] H. Mohsenian-Rad, Optimal bidding, scheduling, and deployment of battery systems in California day-ahead energy market, IEEE Trans. Power Syst. 31 (1) (2016) 442–453, <https://doi.org/10.1109/TPWRS.2015.2394355>.
- [51] S. Shafiee, H. Zareipour, A.M. Knight, Developing bidding and offering curves of a price-maker energy storage facility based on robust optimization, IEEE Trans. Smart Grid 10 (1) (2019) 650–660, <https://doi.org/10.1109/TSG.2017.2749437>.
- [52] T. Ding, Z. Wu, J. Lv, Z. Bie, X. Zhang, Robust co-optimization to energy and ancillary service joint dispatch considering wind power uncertainties in real-time electricity markets, IEEE Trans. Sustain. Energy 7 (4) (2016) 1547–1557, <https://doi.org/10.1109/TSTE.2016.2561967>.
- [53] Y. Wang, Y. Dvorkin, R. Fernández-Blanco, B. Xu, T. Qiu, D.S. Kirschen, Look-ahead bidding strategy for energy storage, IEEE Trans. Sustain. Energy 8 (3) (2017) 1106–1127, <https://doi.org/10.1109/TSTE.2017.2656800>.
- [54] S. Nojavan, A. Najafi-Ghalelou, M. Majidi, K. Zare, Optimal bidding and offering strategies of merchant compressed air energy storage in deregulated electricity market using robust optimization approach, Energy 142 (2018) 250–257, <https://doi.org/10.1016/j.energy.2017.10.028>.
- [55] B. Lin, W. Wu, M. Bai, C. Xie, Liquid air energy storage: price arbitrage operations and sizing optimization in the GB real-time electricity market, Energy Econ. 78 (2019) 647–655, <https://doi.org/10.1016/j.eneco.2018.11.035>.
- [56] A. Akbari-dibavar, et al., Impact of market-driven energy storage system operation on the operational adequacy of wind integrated power systems, Energy 32 (April) (2020), 101731, <https://doi.org/10.1016/j.est.2020.101792>.
- [57] H. Ahmad, A. Akbari Foroud, Improvement of the simultaneous active and reactive power markets pricing and structure, IET Gener. Transm. Distrib. 10 (1) (2016) 81–92, <https://doi.org/10.1049/iet-gtd.2015.0261>.
- [58] M.S. Javadi, et al., A two-stage joint operation and planning model for sizing and siting of electrical energy storage devices considering demand response programs, Int. J. Electr. Power Energy Syst. 138 (2022), 107912, <https://doi.org/10.1016/j.ijepes.2021.107912>.
- [59] H. Mehrjerdi, R. Hemmati, Modeling and optimal scheduling of battery energy storage systems in electric power distribution networks, J. Clean. Prod. 234 (2019) 810–821, <https://doi.org/10.1016/j.jclepro.2019.06.195>.
- [60] R. Rezvanfar, M.Tarafdar Hagh, K. Zare, Power-based distribution locational marginal pricing under high-penetration of distributed energy resources, Int. J. Electr. Power Energy Syst. 123 (May 2019) (2020) 106303, <https://doi.org/10.1016/j.ijepes.2020.106303>.
- [61] A. Soroudi, Power system optimization modeling in GAMS, 2017, <https://doi.org/10.1007/978-3-319-62350-4>.
- [62] A. Hamidi, S. Golshanavaz, D. Nazarpour, in: D-FACTS cooperation in renewable integrated microgrids : a linear multi-objective approach 3029, 2017, pp. 1–9, <https://doi.org/10.1109/TSTE.2017.2723163>, no. c.
- [63] C. Grigg, P. Wong, P. Albrecht, R. Allan, M. Bhavaraju, Q. Chen, The IEEE reliability test system - 1996 - Power Systems, IEEE Transactions on, IEEE Trans. Power Syst. 14 (3) (1999) 11.
- [64] Generalized algebraic modeling systems, “GAMS,” 2021.